Examination of J-Integral methods and their applicability to tough polypropylene materials

Master Thesis

by

Anja Gosch

at

Materials Science and Testing of Polymers

Supervision: Dr.mont. Florian Arbeiter

Assessor: Univ.-Prof. Dr.mont. Gerald Pinter

Leoben, Juni 2017

AFFIDAVIT

I declare in lieu of oath, that I wrote this thesis and performed the associated research myself, using only literature cited in this volume.

EIDESSTATTLICHE ERKLÄRUNG

Ich erkläre an Eides statt, dass ich diese Arbeit selbstständig verfasst, andere als die angegebenen Quellen und Hilfsmittel nicht benutzt und mich auch sonst keiner unerlaubten Hilfsmittel bedient habe.

LEOBEN, Juni 2017

Contents

I. Abstract

To characterize the fracture behaviour of a non linear elastic plastic material, it is common to describe the fracture process with the help of the crack resistance curve. The J-integral represents the difference in potential energy in a linear or nonlinear elastic material, with an infinitesimal difference in crack length (Δa) [1, 2].

Applying the J-Integral to materials which show elastic plastic deformation behaviour requires some preconditions. Hence, several experimental methods exist to determine the crack resistance curve of mentioned non-linear elastic plastic materials. In this study the focus is on the difficulties concerning the application of the load separation method to characterize commercial polymers. Therefore, three different types of polypropylene (PP-H, PP-R and PP-B) were tested. For the characterization of crack resistance the load separation method was used and compared to the more common multi-specimen method [3].

The strong influence of the chosen elastic compliance correction to determine the plastic displacement was examined in detail, since it showed major influence to the load separation curve in the first region (at small plastic displacements/ "unseparable region") and the plateau region (almost constant values of the load separation parameter S_{pb}/ blunting) [3, 4].

In the last region (fracture propagation) all curves show nearly the same slope m_s, regardless of chosen elastic compliance correction. This points toward a key role of the slope ms to indicate the crack advancement produced per unit of plastic displacement in a fracture process, as found in [4].

For comparison multi-specimen tests according to ESIS TC 4 [5] were performed and found to be in the same region as results from the load separation method, for the compliance correction chosen in this work. However, exact determination of crack advancement proved to be difficult, as expected.

II. Kurzfassung

Zur Charakterisierung des Bruchverhaltens von nicht-linear elastisch plastischen Materialien wird üblicherweise eine Risswiderstandskurve (J-R Kurve) verwendet. Das J-Integral repräsentiert die Differenz zwischen der potentiellen Energie bei einem infinitesimalen Rissfortschritt eines linear oder nicht-linear elastischen Materials.

Verwendet man das J-Integral für Materialien welche elastisch plastische Deformationsmechanismen zeigen, so müssen einige Randbedingungen beachtet werden. Daher existieren unterschiedliche Methoden zur Ermittlung einer Risswiderstandskurve von nicht-linear elastisch plastischen Materialien. In dieser Arbeit lag der Fokus bei der“ Load Separation“-Methode und deren Herausforderungen während der Anwendung auf Polymere. Dafür wurden drei unterschiedliche Typen von Polypropylen (PP-H, PP-R und PP-B) untersucht. Zum Vergleich der ermittelten Risswiderstandskurve der „Load Separation“-Methode wurde eine zweite Methode („Multi Specimen“-Methode) verwendet. Der große Einfluss der ausgewählten elastischen Nachgiebigkeit auf die Ergebnisse der Risswiderstandskurve wurde genau untersucht. Vor allem im ersten Bereich der „Load Separation“-Kurve (kleine plastische Deformationen/“unseparable region“) und im Plateau-Bereich (konstante Werte des“ Load Separation“-Parameters) zeigte sich eine große Abhängigkeit von der gewählten elastischen Nachgiebigkeit. Der letzte Bereich der „Load Separation“-Kurve (charakteristisch für stabiles Risswachstum) ist jedoch unabhängig von der gewählten elastischen Nachgiebigkeit. Dies deutet auf eine Schlüssel-Rolle der Steigung m_s im letzten Bereich der „Load Separation“-Methode hin. Die Steigung m_s repräsentiert den auftretenden Rissfortschritt bezogen auf die verursachte plastische Deformation.

Abschließend wurden die Ergebnisse der „Load Separation“-Methode noch mit den Ergebnissen der „Multi Specimen“-Method verglichen. Die Risswiderstandskurven lagen in einem ähnlichen Wertebereich, jedoch stellt eine exakte Charakterisierung des Rissfortschrittes eine Herausforderung dar.

III. Acknowledgment

During the work on this thesis and my studies many people have supported and inspired me and I would like to express my deepest gratitude to them.

First I would like to thank Univ.-Prof.Dr.mont. Gerald Pinter for enabling this thesis and his support as academic supervisor. Furthermore, his really great team for their help in all technical requests.

Very special thanks to my supervisor Dipl.-Ing.Dr.mont. Florian Arbeiter for the possibility to work in one of the in my opinion best groups researching ways of fracture processes in polymers. I´d like to say thank you for the endless discussions about different types of fracture mechanism and on how to determine crack lengths. Thank you for your help in all technical requests and for the opportunity to work nearly without any limitations. I am already looking forward to July where the next big project starts!

I would also like to thank my family who gave me the opportunity to study and for their backing and support in all circumstances. Moreover, I thank my friends and colleagues who are always available when I need them.

1. Theoretical Background

The next chapter deals with the theoretical background necessary for this work. Special focus is put on two methods to characterize the J-Integral (Multi specimen method, Load separation method).

1.1. Elastic plastic fracture mechanics

For materials with a tendency to high plastic deformations, strong non-linearities and high energy dissipation, thus a high material toughness, the use of elastic plastic fracture mechanics is necessary to characterize its toughness. For elastic plastic fracture mechanics the application of the energy based J-Integral, first proposed by Rice in 1968, is a common approach. In general the J-Integral is defined as the required energy per unit area to initialize crack growth in a linear or nonlinear elastic body [6, 7, 8]

Hence it is possible to describe the J-Integral as:

$$J = -\frac{1}{b}\frac{dU}{da}\bigg|_{v} \tag{1.1}$$

where b is the uncracked ligament length, U the potential energy (area under the load displacement record), a the crack length and v the displacement. This expression of the J-Integral extends the linear elastic fracture mechanics towards non-linear material behaviour and large scale plasticity [3, 9, 10].

Furthermore the J-Integral is used to establish the material crack growth resistance curve, the J-R curve. The J-R curve represents the fracture toughness of a material

described by the J-Integral depending on the crack extension Δa. In this case, the measurement of the produced crack extension during testing and the determination of the J-Integral value is necessary [4, 11, 12].

Nevertheless, for a correct application of the J-Integral as a value to characterize elastic plastic fracture mechanics and to construct the crack growth resistance curve (J-R curve) it is important to understand the theoretical background of the J-Integral.

1.2. Theoretical background of the J-Integral

1.2.1. Line integral

The J-Integral is defined as the difference between the external and the internal work, within the area around the notch tip surrounded by a curve Γ for two dimensional problems (see Figure 1.1) [2, 13].

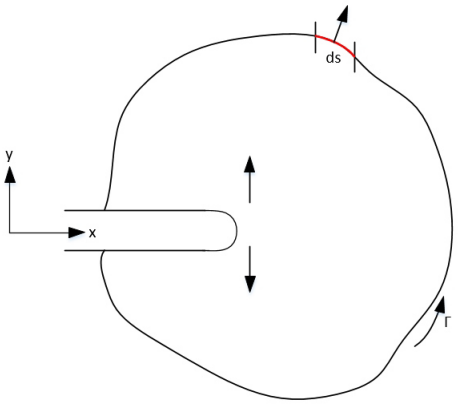

Figure 1.1.: *Definition of the J-Integral surrounding the two dimensional notch tip with a curve according to [2].*

In this case the J-Integral is defined as:

$$J = \int_{\Gamma} w \mathrm{d}y - \int_{\Gamma} T \frac{\mathrm{d}u}{\mathrm{d}x} \mathrm{d}s \tag{1.2}$$

where the external work is expressed by the integration of the strain energy density w along the coordinates and the internal work is defined as the integration of the traction vector T, at the outer side of the integration line Γ, multiplicated with the derivation of the displacement along the x coordinate along the arc length of the integrated curve [2, 8, 14, 15, 16].

The J-Integral, based on the deformation theory, is path-independent, in case the integral includes the whole crack tip (see Figure 1.2). Thus it is no longer important to integrate along the curve from A to C or from F to D for the determination of the J-Integral [17, 18].

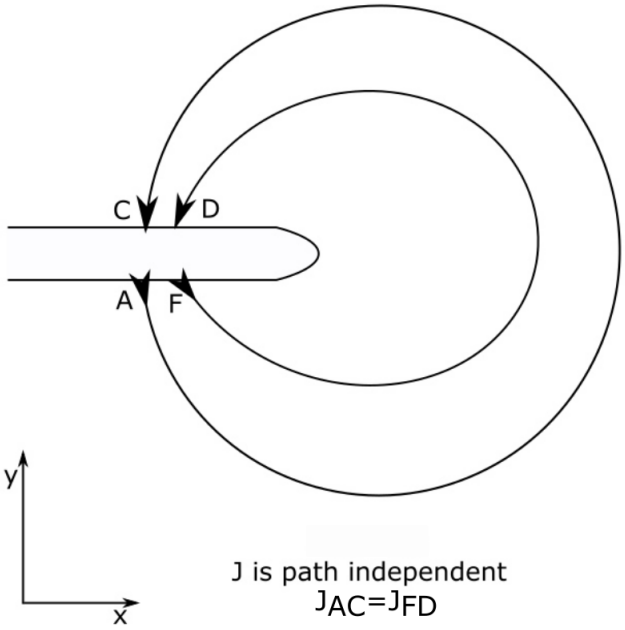

Figure 1.2.: *Path independence of the J-Integral represented with two different integration lines according to [17].*

Now it is possible to write alternative forms of the J-Integral such as:

$$J = \int_0^P \left(\frac{\partial v}{\partial a}\right)_P \mathrm{d}P = -\int_0^v \left(\frac{\partial P}{\partial a}\right)_P \mathrm{d}v \tag{1.3}$$

where, v represents the displacement, P the load and a the crack propagation. These alternative forms are the base for calculating the J-Intagral for various test configura-

tions. In this case the J-Integral is adopted to be a failure criterium and represents a rate of change with respect to crack size a [14, 19].

In general, as long as no crack propagation is detected and purely linear or non linear behaviour occurs, the external applied work is stored elastically and the J-Integral is zero. When the crack propagation starts the J-Integral represents the required energy per unit area to create new surfaces. In other words, the J-Integral is a value to describe the required potential energy in a linear or non linear elastic material to create a small amount of crack propagation (see Figure 1.3). Hence the J-Integral can be described as:

$$J = \frac{1}{B}\frac{\mathrm{d}U}{\mathrm{d}a} \tag{1.4}$$

where U is the total external work, a the crack length and B the specimen thickness.

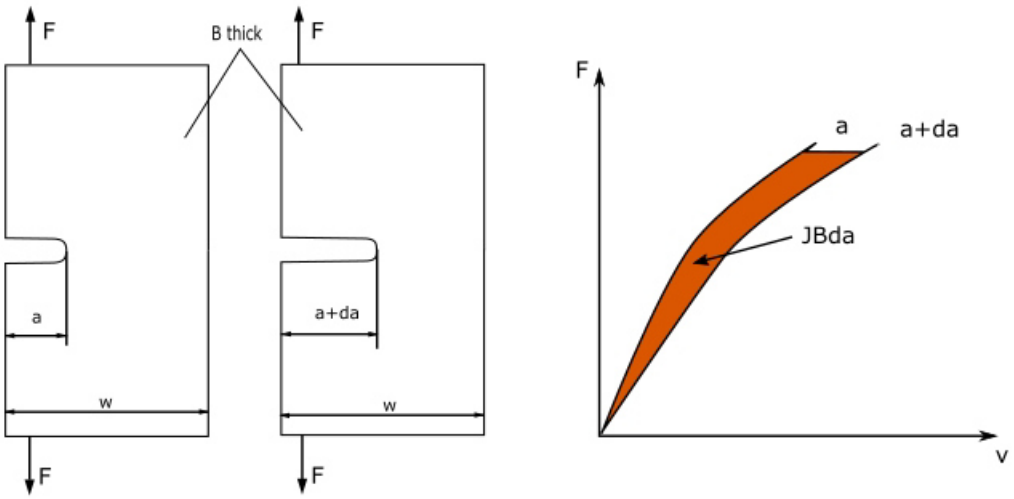

Figure 1.3.: *The J-Integral represents the potential energy to create a small amount of crack growth for linear or non linear elastic material behaviour.*

This definition of the J-Integral has some preconditions concerning the tested specimens [8]:

- deformation in the third direction can be ignored (minimum specimen thickness must be large compared to the yield zone and also the crack length must exceed minimum values)

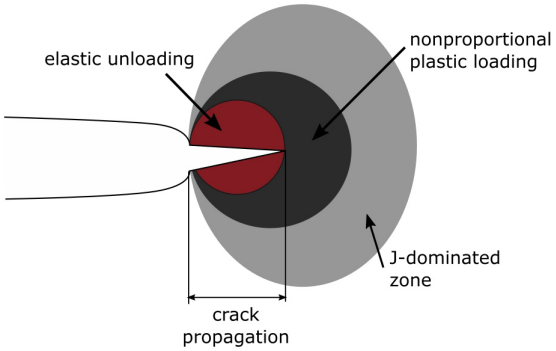

Figure 1.4.: *J-dominated zone in front of the crack tip of a non linear elastic plastic material.*

- material temperature is constant during the testing (otherwise the J-Integral is no longer geometrically independent)
- the load must increase steadily (no unlaoding during the test, which also includes crack propagation where local unloading might occur)

For an elastic plastic material behaviour, the J-Integral does not represent the required potential energy to create a small amount of crack propagation because the conventional J-Integral is based on the deformation theory of plasticity. The J-Integral represents the intensity of the strain and stress dominated field around the crack tip for non linear elastic and elastic plastic materials as shown in Figure 1.4 [20].

Therefore it is possible to connect the J-Integral with the stress intensity factor K_I in the case of small scale yielding:

$$J = \frac{1-\nu^2}{E} K_I^2 \tag{1.5}$$

where E is the Young´s modulus and ν the Poisson´s ratio (see Figure 1.5) [2].

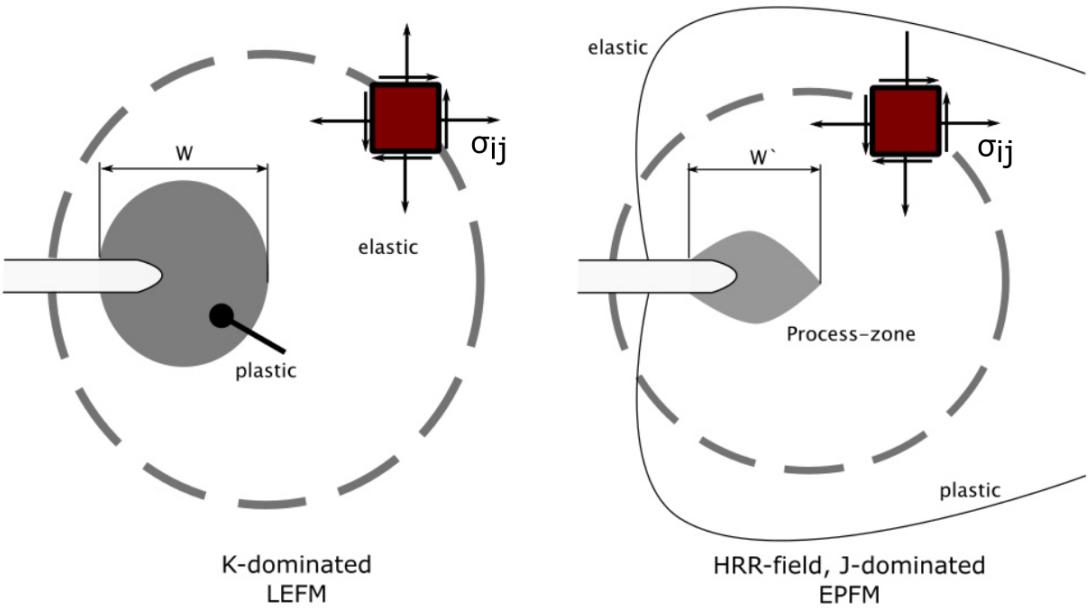

Figure 1.5.: *K-dominated crack tip (linear elastic fracture mechanics LEFM) and J-dominated crack tip (elastic plastic fracture mechanics).*

This connection between the J-Integral and the stress intensity factor K_I is the base for the assumption to describe the crack tip stress field with the help of the first terms of linear elastic or elastic plastic field expansions. In the power-law-hardening crack tip stress field the first term is the HRR-singularity (Hutchinson, Rice and Rosengreen) [2, 21, 22]:

$$\sigma_{ij} = \sigma_0 \left(\frac{J}{I \alpha \epsilon_0 \sigma_0 r} \right)^{\frac{1}{1+n}} \sigma_{ij}^{(1)}(\rho) \tag{1.6}$$

where J is the path independent J-Integral. In the case of linear elastic material behaviour, the crack tip stress field for mode I is given by [23]:

$$\sigma_{ij}(r,\rho) = \frac{K_I}{\sqrt{2\pi}} r^{-1/2} f_{ij}^{(1)}(\rho) + T_{stress} r^0 f_{ij}^{(2)}(\rho) + ... \tag{1.7}$$

where K_I is the stress intensity factor. Based on the equation concepts of linear elastic fracture mechanics and elastic plastic fracture mechanics both show a dominance

requirement for the first singular term characterized by the stress intensity factor K and the J-Integral [22].

Therefore it is possible to detect a J-controlled crack growth with the help of the stress field around the crack tip. Figure 1.6 shows three different types of crack tip with their typical stress field. The stress field of a small scale yielding crack tip can be described with the help of linear elastic fracture mechanics (LEFM) and with the HRR-field (non linear elastic plastic J-Integral) and hence is characterized as J-controlled crack growth. Additionally it is possible to describe the crack tip under elastic plastic conditions with the help of the HRR-field and thus is also characterized as J-controlled crack growth. However it is not possible to describe the last crack tip (large strain region) with any stress field and this ends up in no J-controlled crack growth.

The application of the J-Integral is connected with restrictions when it is applied for elastic plastic materials. For the correct use of the J-Integral the conditions of proportional loading have to be fulfilled, e.g. no unloading process in the material during testing. These unloading processes occur due to the formation of voids in front of the crack tip or due to crack extension. Secondly the J-Integral does not describe the crack driving force for elastic plastic materials, only the intensity of the crack tip field. In this case the J-Integral describes the intensity of the crack tip field even for a limited crack extension, but only as long as the conditions of "J-controlled crack growth" are fulfilled (see Figure 1.4). Therefore the J-Integral is not representative for materials with large crack growth or in the case of cyclic loading [25].

The application of the defined J-Integral is only possible for plain strain conditions. To achieve plain strain testing conditions, there are some requirements for the test specimens and the testing itself. First a minimal specimen thickness compared to the yield zone must exist. Furthermore, the crack length and the notch tip also have to have fixed values with regards to the specimen geometry. The J-Integral is only valid if there are no kinetic effects, for example at low speed testing conditions. It is not possible to detect the J-Integral of a material when the material temperature is

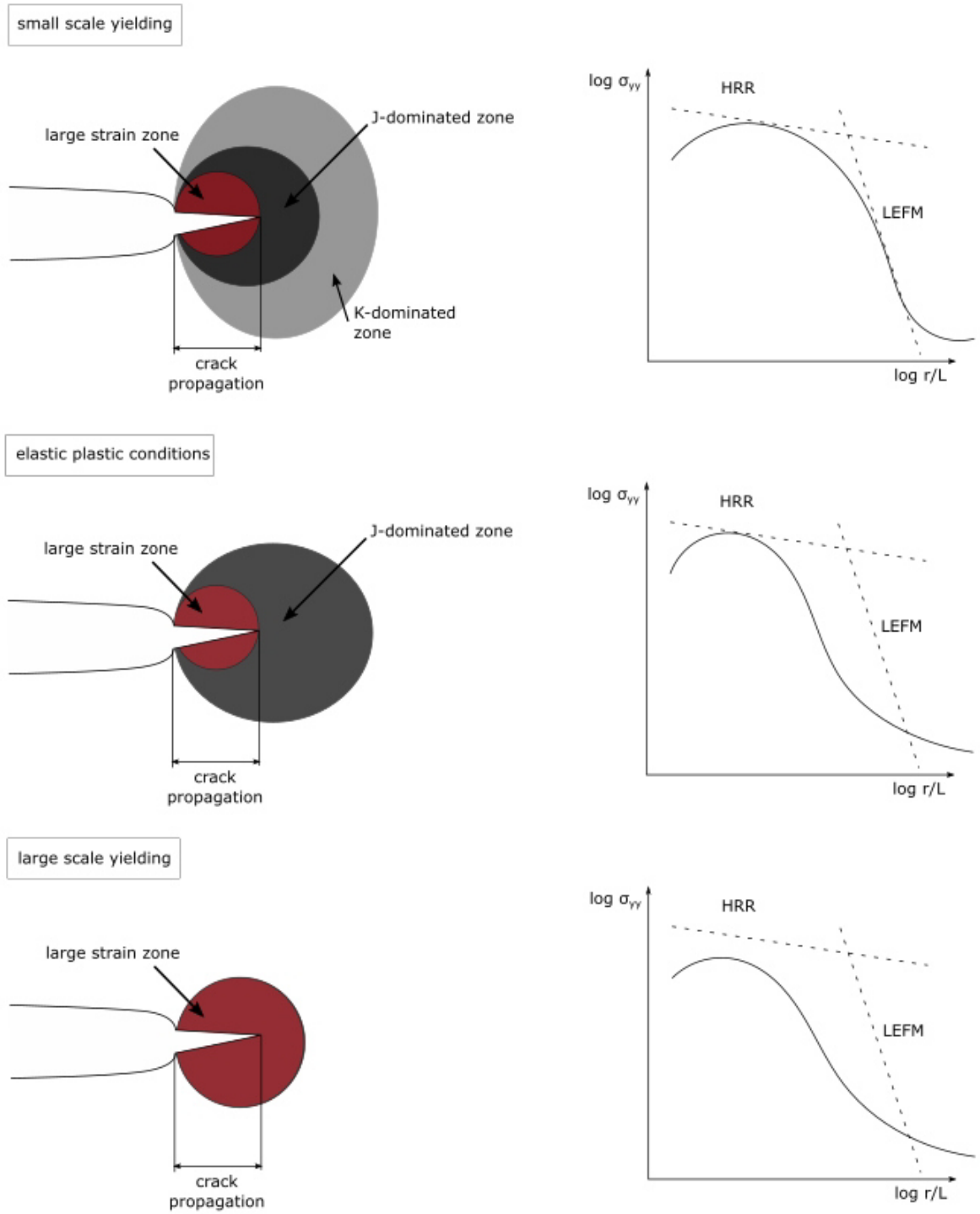

Figure 1.6.: *Stress field around the crack tip for small scale yielding, elastic palstic conditions and large scale yielding according to [24].*

not constant or thermal effects occur. Additionally the load has to increase steadily during testing [8].

Concerning the practical application of the J-Integral there exists several procedures and methods to create a fracture resistance parameter for ductile polymers. The basic approach concerning the J-Integral was done for metals with the construction of the crack resistance curve (J-Δa-curve) with the help of the multi specimen method proposed by ASTM. But there are also several normalization procedures to determine the J-Integral. In the next section some methods and procedures are presented to calculate the J-Integral [6].

1.3. Practical application of the J-Integral

It is common to use the J_{IC} parameter to characterize the plane-strain fracture resistance of ductile polymers. The J_{IC} parameter is connected with the initiation during fracture and calculated from the load displacement record. Experimentally it is challenging to characterize the point of physical fracture initiation, but once the initiation point is set the J_{IC} parameter can be calculated easily with the help of the single specimen J-form [6]:

$$J = \frac{\eta U}{B(W - a_0)} \tag{1.8}$$

where U is the area under the load displacement curve, η is a calibration factor, W is the specimen width, B the specimen thickness and a_0 the initial crack length.

1.3.1. Multi specimen method

For the construction of the material crack growth resistance curve (J-R curve, J-Integral depending on the crack propagation Δa) it is common to use the multi specimen method. The currently common procedure was developed by the Technical Committee 4 of the European Structural Integrity Society, ESIS TC4, on "Polymers and Polymer Composites". Within the multi specimen method, several identical specimens

are loaded up to different displacements without complete fracturing and unloaded immediately afterwards. The measured load P versus displacement v plots for the tested specimens are shown in Figure 1.7. To determine the initial and final stable crack lengths the tested specimens get cooled with liquid nitrogen and cryo fractured. The generated crack lengths can be measured directly from the crack surface with optical devices. Now it is possible to calculate the related J-Integral for every crack length and the crack resistance curve can be constructed (see Figure 1.7). Generally this method has a very high material consumption and the sample preparation is also extremely time consuming. Furthermore, results of this method are strongly influenced by the optical measurement of the crack surface [4, 5, 11].

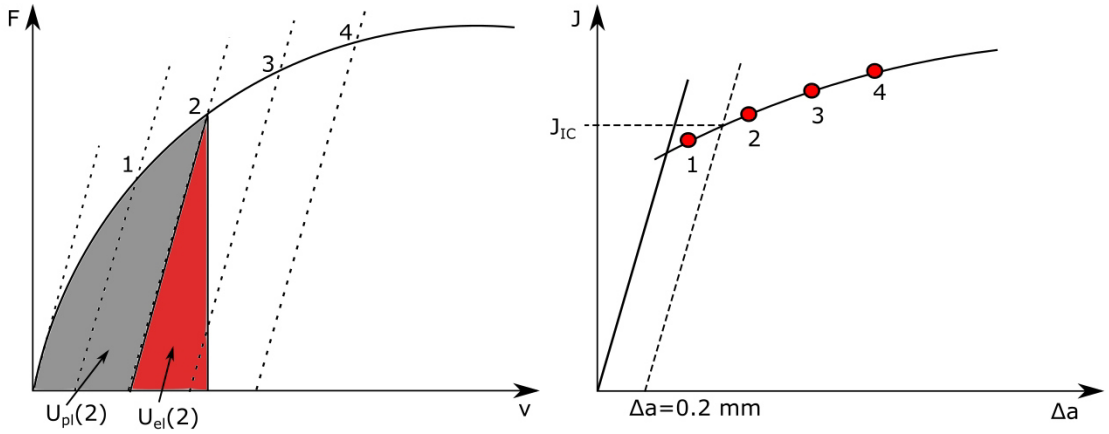

Figure 1.7.: *Procedure to create a crack resistance curve via the multi specimen method. Measurement of load-displacement records of various specimens and calculated J-R curve at different crack growths Δa according to [8].*

During the fracture process there is one characteristic plastic deformation process at the beginning called "blunting-mechanism". The blunting mechanism is shown in Figure 1.8 where a sharp notched specimen gets loaded and before the crack starts to propagate the crack tip shows a round notch and large stress concentrations. During the blunting process the crack advancement occurs through the formation of a "stretch-zone". Especially soft polymers tend to crack tip blunting because of their

high cohesive strength compared to the elastic modulus. The identification of the blunting process is difficulty but in general the blunting line is given as:

$$J_{IC} = 2\sigma_y \Delta a \tag{1.9}$$

where σ_y is the yield stress. The J_{IC} value is defined as the intersection of the J-R-curve and a 0.2 mm offset in the blunting line (see Figure 1.7) [26].

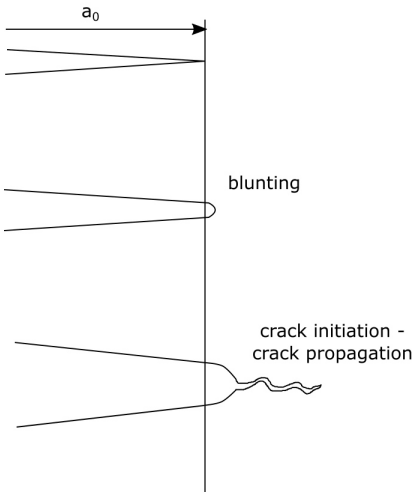

Figure 1.8.: *Blunting mechanism of the crack tip at the beginning of the fracture process [26].*

1.3.2. Challenges of the multi specimen method

Measurement of the crack length

The characterization of the actual crack growth during J-Integral experiments is one of the major challenges. While the initial crack length can be determined easily by optical measurement devices, the determination of the crack propagation during the fracture process is difficult and has a major influence on the resulting values of the crack resistance curve. The reliability of the direct observations of the crack front depends strongly on the material under investigation and the testing conditions. It is hard to detect the starting point of fracture propagation on an opaque material where the specimens are thick enough to reach plane strain conditions. Furthermore it is also

complicated to detect the crack initiation in transparent polymers by visual distortion and crack tunnelling. In general the crack propagation process itself is very complex and it is possible that there is more than one deformation mechanism at the same time. There exist different methods to determine the location of the crack front. One method is to cool the tested specimens with liquid nitrogen and break the specimen with the help of impact tests. Another one is to break up the tested specimens only by high rate impact fracture or fatigue cyclic loading. All these methods require the optical measurement in a second step to identify the crack front. In some cases it is common to inject ink at the end of the fracture test to mark the fracture propagation. This procedure can help to identify the crack front easier. But not for all materials the marking of the fracture surface with ink results in a correct validation of the crack front because there are some deformation mechanisms like crazes who can distort the measurement. Additionally there exists a method to measure the crack front on a polished section of the test specimen under load [6, 8].

Initiation toughness parameter

It is very difficult to detect a clear transition from the crack blunting phase to the fracture propagation. Hence, a pseudo initiation fracture resistance parameter $J_{0.2}$ (Δa = 0.2 mm) has been introduced to identify the point of crack initiation. The chosen value of 0.2 mm is small enough to be close to the point where the crack becomes instable and the fracture propagation starts but large enough for experimental measurement [6, 7, 8].

1.3.3. Single specimen method

The development of new indirect methods to characterize the crack resistance curve of ductile polymers is strongly promoted because of the very time consuming experimental procedure of the multi specimen approach. According to literature [6], Sharobeam and Landes presented an experimental procedure based on the load separation principle to construct the material resistance curve of an elastic plastic material.

Additionally, it is possible to characterize the crack blunting phase and the point of fracture initiation before the construction of the material resistance curve. The load separation method deals with two different sorts of testing specimens, the single pre-cracked specimen, and a blunt notched specimen to determine the J-Integral depending on the crack extension. The load separation criterion describes the load depending on two functions, the geometry and the load function of the tested material. Based on these theoretical conditions the load separation parameter S_{pb} is defined as a ratio of the load of the pre-cracked specimen to the load of the blunt notched specimen. The load separation parameter S_{pb} is depending on the plastic displacement of the tested specimen. In general, no crack growth in the blunt notched specimen is allowed to achieve a correct load separation curve. Furthermore, stable crack growth in the pre-cracked specimen is necessary. With the help of the load separation curve it is possible to determine the crack initiation point. Another advantage is the independence of the load separation curve from the deformation function and the crack tip blunting in the specimen during testing [6, 11, 27].

Theoretical background of the load separation method

Generally the J-Integral is defined as a parameter for characterizing the plain strain fracture resistance of ductile polymers. The load separation principle displays another form of the J-Integral, split up in an elastic and a plastic part [6, 12, 19, 28]:

$$J = J_{el} + J_{pl}. \tag{1.10}$$

The elastic J-Integral J_{el} can be determined by using parameters from the Linear elastic fracture mechanics (LEFM) and the plastic J-integral J_{pl} is expressed by:

$$J_{pl} = \eta_{pl} \frac{A_{pl}}{b} \tag{1.11}$$

where A_{pl} represents the area under the load per unit thickness vs plastic displacement record, b is the uncracked ligament length of the body and η_{pl} is a geometry dependent factor [12].

There is another representation of the J-Integral. The generalisation of the single specimen technique. In this representation, the J-Integral is divided in an elastic and a plastic component (Rice, Sumper and Turner) [6, 29]:

$$J = \eta_{el}\frac{A_{el}}{b} + \eta_{pl}\frac{A_{pl}}{b} \tag{1.12}$$

Where A is the area under the load displacement record and η a function of the crack length to width ratio a/W [6, 29].

The elastic component of the J-Integral can be replaced by the standard test methods for J_{IC} (plain strain fracture toughness in mode I) [3]:

$$J = \frac{K^2}{E} + \eta_{pl}\frac{A_{pl}}{b} \tag{1.13}$$

where K is the stress intensity factor, determined by the help of linear elastic fracture mechanics.

The possibility to separate the J-Integral in an elastic and a plastic part is the basic assumption for the load separation principle.

Load separation principle

The load separation principle is based on the assumption, that the load P is a function of the crack length a and the plastic displacement v_{pl}, for tested specimens of the same material, geometry and constraint. This is mathematically written as the multiplication of the geometry function g and the deformation function H [3, 14, 29, 30]:

$$P = g\left(\frac{a}{W}\right)H\left(\frac{v_{pl}}{W}\right). \tag{1.14}$$

The plastic displacement v_{pl} is determined by subtracting the elastic displacement v_{el} from the displacement during testing:

$$v_{pl} = v - v_{el} = v - CP \tag{1.15}$$

where C is the elastic compliance of the specimen (with ligament length b and width W) and P the load [6].

In a next step the load separation parameter S_{pb} is constructed as a ratio of the load of the sharp notched specimen to the load of the blunt notched specimen at the same plastic displacement:

$$S_{sb}(v_{pl}) = \left.\frac{P_s}{P_b}\right|_{v_{pl}} \tag{1.16}$$

An example for a typical load separation parameter curve is shown in Figure 1.9 (load separation parameter S_{pb} depending on the plastic displacement v_{pl}).

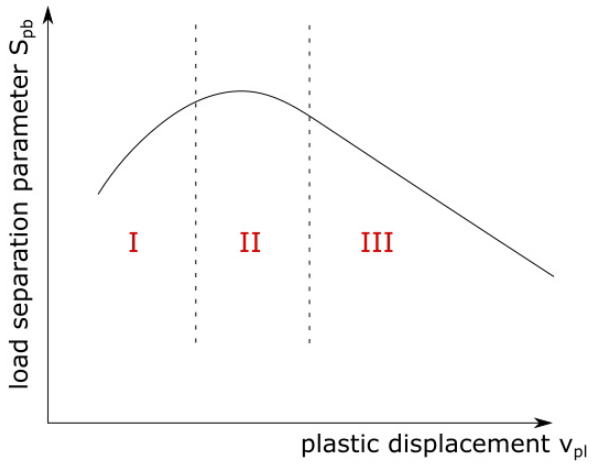

Figure 1.9.: *Load separation parameter S_{pb} depending on the plastic displacement v_{pl} with three typical regions within this curve (I,II,III).*

The load separation principle is verified for stationary crack propagation, in this case it is possible to expand to specimens with fracture propagation, which will be discussed lateron [4, 6, 11, 29].

In general the load separation parameter shows three characteristic regions (see Figure 1.9) the early region of plastic displacement (region I), also named the “un-

separable" region. Where no load separation is possible because the S_{pb} parameter is highly unstable. This region is followed by a constant region, the "plateau" region (region II), characterized by a constant plateau, representing the blunting process of the sharp notched specimen. The last region, where the load separation parameter decays (region III) is characteristic for "fracture propagation" and corresponds to the fracture process in the sharp notched specimen [4, 6, 29].

For bending testing conditions, the geometry function g can be written as the ratio of b ($b = W - a$) to the specimen width W to the power of two [29]:

$$G = (b/W)^2. \tag{1.17}$$

The deformation function H can be estimated by normalising the test records by the geometry function g:

$$P_N = \frac{P}{W^2 G(a/W)} = H(v_{pl}/W) \tag{1.18}$$

where P_N is the normalised load and represents the characteristics of the crack tip geometry. Based on this equation it is possible to write a functional form of the normalised load P_N as a simple power law function:

$$P_N = \beta(v_{pl}/W)^n \tag{1.19}$$

There exists a slight modification of this power law, because the separation assumption is only valid above a lower limit of plastic displacement $v_{pl,min}$ [29]:

$$P_N = P_N - P_{N0} = \beta\left(\frac{v_{pl} - v_{pl,min}}{W}\right)^n = \beta\left(\frac{v'_{pl}}{W}\right)^n \tag{1.20}$$

Load separation in stationary cracks

If it is possible to describe the load, for a given material, geometry and constraint, in a separable form, the load separation parameter S_{ij} can be constructed. As discussed

before, the load separation parameter S_{ij} is defined as ratio of the load $P(a_i)/P(a_j)$ at the same plastic displacement v_{pl}, for different stationary crack lengths a_i and a_j [3]:

$$P = G\left(\frac{a}{W}\right)H\left(\frac{v_{pl}}{W}\right). \tag{1.21}$$

$$S_{ij} = \left.\frac{P(a_i)}{P(a_j)}\right|_{v_{pl}} \tag{1.22}$$

$$S_{ij} = \frac{G(a_i/W)}{G(a_j/W)} \tag{1.23}$$

For fixed values of a_i and a_j the geometry function is constant and as a result, the separation parameter S_{ij} is a constant value and no function of the plastic displacement v_{pl}. Therefore, a constant separation parameter S_{ij} at stationary crack growth implies a separable form of the load [3].

Load separation in growing cracks

The load separation principle can be extended to growing cracks. Once more the load can be written as a combination of a geometry function G and a deformation function H, for the same material, geometry and constraints [3]:

$$P = G_p(b_p/W)H_p(v_{pl}/W). \tag{1.24}$$

In a second step the load is normalized by a ratio of the load P_p of the pre-cracked (sharp notched) specimen to the load P_b of the blunt notched specimen.

$$\frac{P_p}{P_b} = \frac{G_p(b_p/W)H_p(v_{pl}/W)}{G_b(b_b/W)H_b(v_{pl}/W)} \tag{1.25}$$

Based on this normalization the load separation parameter can be constructed. The indices of the load separation parameter S_{pb} refer to the definition of the parameter,

as a ratio of the load of a pre-cracked specimen (sharp notched specimen) to the load of a blunt notched specimen at the same plastic displacement [3]:

$$S_{pb} = \left.\frac{P_p}{P_b}\right|_{v_{pl}} \tag{1.26}$$

$$S_{pb} = C_3 G_p(b_p/W) H_{pb}(v_{pl}/W) \tag{1.27}$$

The geometry function of the blunt notched specimen G_b is constant and substituted by the parameter C_3, where C_3 is $1/G_b$. Furthermore the deformation functions are summarized in one parameter H_{pb} representing the ratio of the deformation function of the pre-cracked specimen and the deformation function of the blunt notched specimen at the same plastic displacement. It was found that the separation parameter is independent of the plastic displacement and therefore independent of the deformation function and the load separation parameter S_{pb}. Which can be represented only by the geometry function for growing crack measure [3]:

$$S_{pb} = C_3 G(b_p/W) \tag{1.28}$$

In a next step, the geometry function g, can be written as a power law function $A(a/W)^m$. The specimen width W and a constant A which is equal at the pre-cracked and blunt notched specimen and the load separation parameter S_{pb} can be written as a function of the crack length a [3, 11]:

$$S_{pb} = \left.\frac{P_p(a_p, v_{pl})}{P_b(a_b, v_{pl})}\right|_{v_{pl}} = \left.\frac{g_p(\frac{a_p}{W}) H(\frac{v_{pl}}{W})}{g_b(\frac{a_b}{W}) H(\frac{v_{pl}}{W})}\right|_{v_{pl}} = \frac{g_p(\frac{a_p}{W})}{g_b(\frac{a_b}{W})} = \frac{A(\frac{a_p}{W})^m}{A(\frac{a_b}{W})^m} = \left.\left(\frac{a_p}{a_b}\right)^m\right|_{v_{pl}} \tag{1.29}$$

where a_p is the crack length of the pre-cracked specimen and a_b the notch length of the blunt notched specimen. The variation of the load separation parameter S_{pb} is related to the crack propagation in the pre-cracked specimen. Therefore it is possible

to estimate the crack propagation in the pre-cracked specimen during testing by the load separation parameter [11, 31]:

$$a_p = a_b \left(\frac{P_p}{P_b} \right)^{1/m} = a_b (S_{pb})^{1/m} \tag{1.30}$$

The crack length can be determined for every point of the load displacement record if m is known. To calculate m calibration points are needed. There should be no crack propagation in the blunt notched specimen meaning a_b is constant during the whole test, whereas the pre-cracked specimen shows an increasing crack length a_p. After testing it is possible to measure the initial crack length a_{p0} and the final crack length a_{pf} on the fracture surface of the pre-cracked specimen. But the determination of the final crack length a_p is not always that easy and clear as discussed before. Hence, a theoretical calibration point is calculated. The load of the blunt notched specimen P_b and the load of the pre-cracked specimen P_p is assumed to be the same when the crack lengths show the same value, thus the load separation parameter S_{pb} is equal to 1 [11]:

$$a_p = a_b, P_p = P_b \tag{1.31}$$

$$S_{pb} = \left. \frac{P_p}{P_b} \right|_{v_{pl}} = \left(\frac{a_p}{a_b} \right)^m = 1 \tag{1.32}$$

The theoretical calibration point is especially useful for tested specimens where it is impossible to determine the final crack length [11, 32].

Now the crack propagation Δa in the pre-cracked specimen at every point of the load vs displacement record is known and it is possible to calculate the J-Integral

$$J_0 = \frac{\eta U}{B(W - a_0)} \tag{1.33}$$

where η is a geometry dependent factor (η = 2 for single edged notched bending specimens, SENB and η = 2+ 0.552(1-a_0/W) for compact tension specimens, CT), U is the area under the load displacement record, B is the specimen thickness, W is the

specimen width and a_0 the initial crack length. Finally, there is a correction required to account for the crack growth during the measurement which would otherwise not be allowed, according to the definition of the J-Integral:

$$J = J_0 \left[1 - \frac{(0.75\eta - 1)\Delta a}{W - a_0} \right] \tag{1.34}$$

1.3.4. Challenges of the single specimen method

One of the major advantages by the use of the single specimen method to determine the crack resistance curve is the continuous characterization of the crack propagation during testing. But it is worth pointing out that, there are a lot of influencing factors for a correct determination of the load separation method [4].

First of all the calculation of the elastic compliance value C to determine the plastic displacement v_{pl} according to Equation 1.15. The chosen elastic compliance value directly influences the plastic displacement value and hence, the load separation parameter S_{pb} [4].

Furthermore the starting point of fracture propagation characterized by the maximum value of the load separation curve influences the crack resistance curve. For the determination of the fracture initiation exist different methods and in some cases it is necessary to verify the results of the load separation method with the help of the multi specimen method. A visual inspection of the crack surface of different tested specimens with a very small crack extension should help to identify the starting point of fracture propagation [4].

In conclusion, the characterization of non linear elastic plastic fracture behaviour is challenging and requires a lot of testing knowledge. There exists many influencing factors from the testing procedure and the method itself. Hence, the determination of further parameters to characterize the fracture propagation of a non linear elastic material behaviour is going on. Concerning the load separation method there exists a parameter m_s to classify the fracture propagation process by the amount of crack

growth produced in the plastic region according to literature [4]. This parameter is also used in this study to rank the tested tough types of polypropylene.

2. Experimental

2.1. Testing configurations

2.1.1. Description of the used materials

This work focuses on the characterization of crack growth behaviour of extremely tough materials. Therefore three different types of Poylpropylene were used. The aim was to ascertain a crack growth parameter (in this work the J-Integral) to rank tough materials concerning their fracture behaviour. Table 2.1 gives an overview about the used material types in this study according to literature [33].

Shortcut	Material	Young's Modulus	Yield Stress	Density	MFR
		23°C (MPa)	23°C (MPa)	23°C (kg/m³)	230°C/2.16kg (g/10min)
PP-H	Polypropylene Homopolymer	1650	36	905	0.3
PP-R	Polypropylene Randomcopolymer	900	25	905	0.25
PP-B	Polypropylene Blockcopolymer	1300	28	900	0.3

Figure 2.1.: *Types of used Polypropylene with their field of application and material data according to [33].*

Furthermore these materials were characterized in dynamic-mechanical analysis (DMA) measurements. The damping behaviour of PP-H and PP-B is rather similar whereby PP-R show a slightly higher level. Additionally, the properties of PP-R changes more significantly at higher temperatures which can be explained by the onset of melting temperature, as determined via differential scanning calorimetry (DSC)

measurements. Additionally, the morphology of the used Polypropylene materials was investigated using microtome slices and a polarized light microscopy with a magnification of x500. Formations of spherulites, most likely in α -modification were detected for PP-H. PP-R shows a slightly different appearance of spherulitic formations. The morphology of PP-B shows incorporated ethylene blocks. Moreover the molecular mass distribution was determined for the used Poylpropylene types. The lowest number average molar mass show PP-B (89,000) compared to PP-R (91,300) and PP-H (111,000). The mass average molar mass was the highest for PP-B (605,000), followed by PP-R (538,000) and PP-H (557,000). In general the used materials show comparable molecular weight and distribution. Therefore it is necessary to characterize the influence of different morphology on the fracture mechanisms of the used Polypropylene types. Because of the extremely tough material behaviour the fracture mechanism exceeds the preconditions of linear elastic fracture mechanics under monotonic loading and the methods of non linear elastic plastic fracture mechanics (in this study the J-Integral) are necessary [33].

2.1.2. Specimen geometry and specimen preparation

In order to characterize the fracture resistance curve the different materials were tested in a three point bending configuration. Therefore, a SENB specimen geometry (single edged notched bending) was used. The detailed specimen geometry is shown in Figure 2.2. Generally the specimen width W was taken as the maximum available value (limited by availability of compression molded sheets) and the other geometry parameters are derived from the specimen width W [8].

An important part of the specimen preparation is the notching. Hence the crack tip radius and the notch quality are essential parameters for the determination of the fracture toughness via elastic plastic fracture mechanics. There are several methods to create a sharp notch, e.g. by a natural crack by fatigue cracking or with the help of a razor blade. Generally the resulting crack tip radius must be lower than 20 μm. The notching process and therefore also the chosen sharpening method influence not

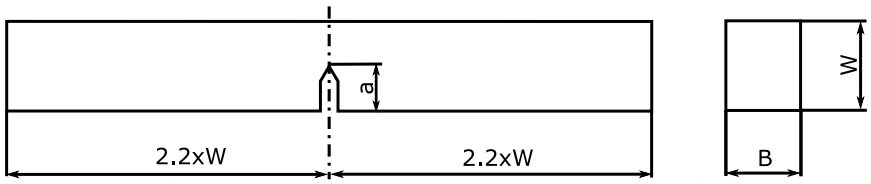

Geometriedaten	
W	16 mm
B	6,4 mm
a	8,8 mm

Figure 2.2.: *Used specimen geometry SENB (Single edged notched bending) according to [8].*

only the crack growth initiation parameter, but affect the whole fracture process. The sharpening process was made with a razor blade pushed into the root of the V-notch of the specimen [34].

The initial crack length a_0 of every specimen was detected directly on the fracture surface after testing and cryofracturing with the help of a microscope. Generally the initial crack length Δa should satisfy the requirement [8]:

$$0.55 \leq a_0/W \leq 0.65 \tag{2.1}$$

2.1.3. Testing conditions

The SENB specimens were tested in bending configuration (see Figure 2.3) with a constant loading rate of 1mm/min at room temperature. The application of side-grooves was intentionally forgone in order to be able to better monitor the formation of plastic deformation and crack propagation on the specimen surface, for a better understanding of the fracture process of the materials in question [8].

2.1.4. Crack length measurement

The crack resistance curve is strongly influenced by the crack length measurement. The determination of the initial crack length a_0 and the final crack length a_f are done directly on the fracture surface of the tested specimens. Generally the measurement

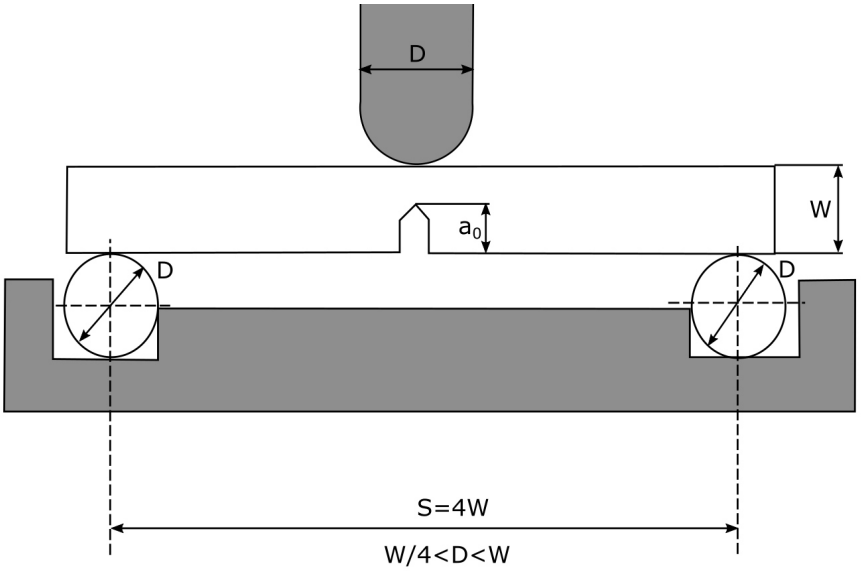

Figure 2.3.: *Testing conditions in bending according to [8].*

of the initial crack length a_0 is less erroneous to the final crack length a_f. In some cases the crack front is difficult to detect and therefore its exact shape and the location of the crack front is subjective and prone to errors. Hence, it is important to gain experience in characterizing the crack growth Δa for each individual material. Figure 2.4 shows a schematic crack surface of a tested specimen and illustrates the difficulties of the determination of the crack propagation. Because the crack growth Δa is an average value and not as clear as the crack front of the fracture propagation.

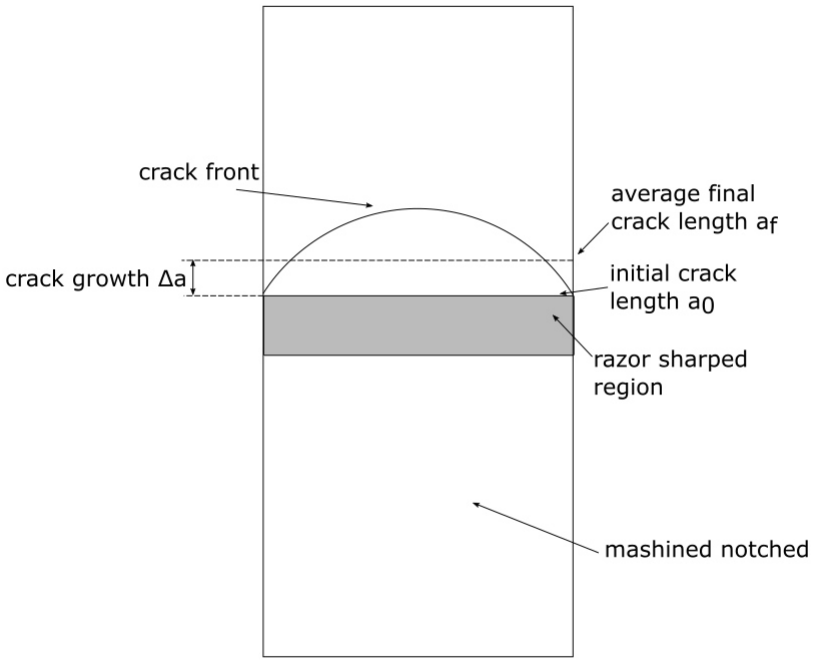

Figure 2.4.: *Measuring of the crack front on the cracked surface according to [8].*

2.2. Multi specimen method

One method which was applied to characterize the crack resistance curve is with the multi specimen method, where several test specimens are deformed up to different displacements and afterwards directly unloaded before a complete fracture of the specimen. By applying this procedure, different crack growths are induced in the loaded specimens. After testing, specimens were cryo fractured to determine the crack length as described before. Hence it is possible to calculate the fracture resistance J_0, where no crack growth can be measured, for every tested specimen [4, 6, 8]:

$$J_0 = \frac{\eta U}{B(W - a_0)} \tag{2.2}$$

where η is 2 for SENB specimen, B is the specimen thickness, W the specimen width, a_0 the initial crack length and U represents the area under the load versus displacement record (absorbed energy).

During the determination of the absorbed energy U, it is necessary to correct the absorbed energy U to lower values because of indentation effects during the measurement (pin penetration, machine stiffness, etc). Thereby an unnotched sample is loaded with the same loading conditions as the notched samples and the absorbed energy U_{corr} of the unnotched sample is subtracted from the absorbed energy U_0 of the tested specimen (indentation correction).

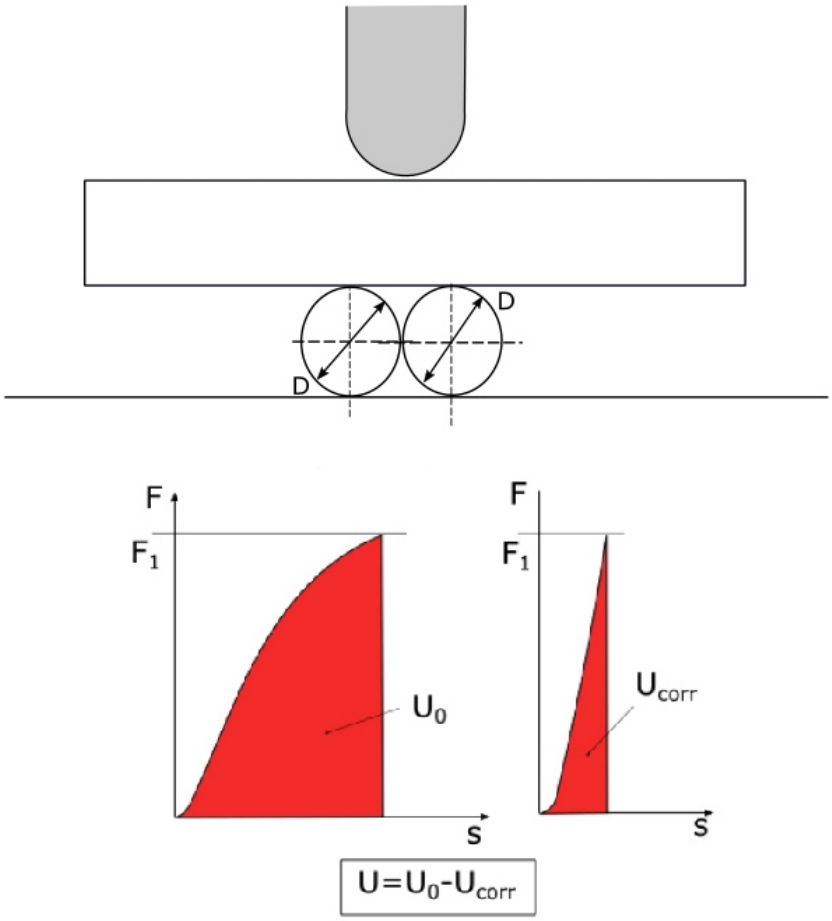

Figure 2.5.: *Test setup to determine the indetation correction according to [8].*

At this point, it is possible to determine the actual crack growth Δa of every specimen e.g. via microscopic analysis as stated before. Therefore, the initial crack length a_0 is subtracted from the final crack length a_f as in Formula 2.3.

$$\Delta a = a_f - a_0 \tag{2.3}$$

With the determined actual crack growth Δa the calculated J_0 can be corrected for the amount of actual crack propagation in the specimen. For this purpose, the calculated J_0 is used to calculate the J-Integral as a function of crack propagation Δa [34]:

$$J = J_0 \left[1 - \frac{(0,75\eta - 1)\Delta a}{W - a_0} \right] \tag{2.4}$$

In a next step it is possible to construct the crack growth resistance curve where the J-Integral depends on the determined crack growth Δa.

2.3. Load separation method

Secondly the crack resistance curve (J-Δa-curve) was determined with aonther experimental procedure according to the load separation method. The principle of the load separation was discussed in detail in the theoretical part [4, 6, 11, 6, 34].

2.3.1. Specimen preparation for the load separation method

The specimen configuration of the load separation method is different compared to the multi specimen method. There are two types of specimens used for the application of the load separation method. The sharp notched specimen sN also called precracked specimen, and the blunt notched specimen bN. The sharp notched specimen is the same specimen type as used for the multi specimen method, and also sharpend with the same technique. The blunt notched specimen showed a round notch with a radius bigger than 0.5 mm [11].

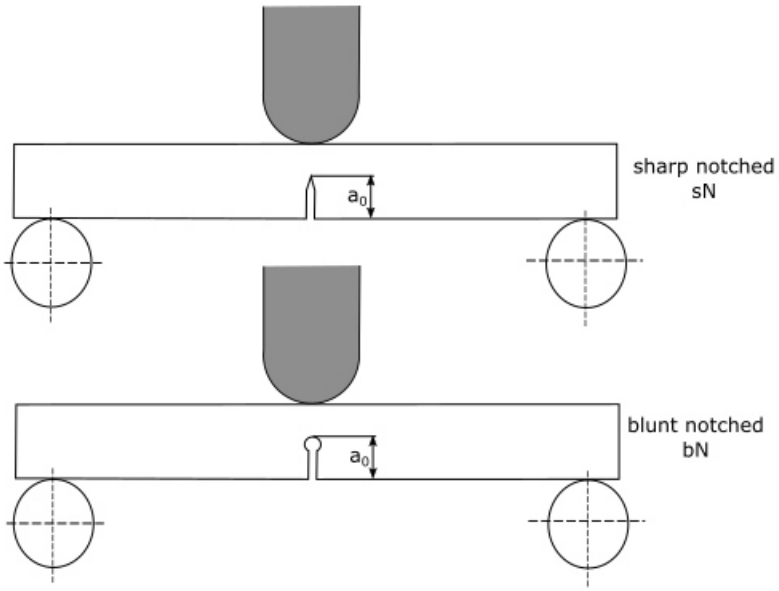

Figure 2.6.: *Specimen configuration sharp notched sN and blunt notched bN specimen according to [4]*

2.3.2. Testing procedure

The testing procedure of the load separation method is similar to the multi specimen method, but less specimens are needed. The sharp notched and the blunt notched specimens are both loaded in bending configuration. Whereas a crack starts to propagate in the sharp notched specimen, no crack propagation is allowed in the blunt notched specimen. This testing procedure also allows no complete fracture of the sharp notchted specimen. After testing the specimens were completely fractured in liquid nitrogen to determine the crack propagation on the fracture surface of the specimens as discussed before. The result of the test is a load versus displacement curve of the sharp notched and the blunt notched specimen [11].

2.3.3. Calculations of crack length and evaluation of the J-Integral

For the application of the load separation method the measured load P versus displacement v curves are adapted to load P versus plastic displacement v_{pl} curves. Therefore the plastic displacement v_{pl} is determined as

$$v_{pl} = v - v_{el} = v - CP \tag{2.5}$$

where v is the measured displacement from the testing machine, v_{el} is the elastic displacement and C is the initial compliance. The initial compliance C and the load P represent the elastic part of the displacement [34].

Now it is possible to evaluate the load separation parameter S_{pb}. Therefore

$$S_{pb} = \left.\frac{P_p}{P_b}\right|_{v_{pl}} \tag{2.6}$$

where P_p is the load of the sharp notched specimen and P_b is the load of the blunt notched specimen at the same plastic displacement v_{pl}. As discussed in the theoretical part of this work the load separation parameter S_{pb} represents the crack propagation a_p in the sharp notched specimen with regard to the initial crack length in the blunt notched specimen a_b and a parameter m. This relation is defined as:

$$S_{pb} = \left.\frac{a_p}{a_b}^m\right|_{v_{pl}} \tag{2.7}$$

where the crack lengths in the sharp notched (a_p) and the blunt notched specimen (a_b) are connected with the parameter m at the same plastic displacement v_{pl}.

Hence, it is necessary to calculate the exponent m for a determination of the crack length in the sharp notched specimen with:

$$m = \frac{log(S_{pb})}{log(a_p/a_b)} \tag{2.8}$$

For a correct calculation of the exponent m a point of the load separation curve for which the crack length in the sharp notched specimen (a_p), the crack length in the blunt notched specimen (a_b) and the correct value of the load separation parameter S_{pb} is known must be used. These calibration points are at the beginning of the crack propagation (region II of the load separation curve) and at the end of the load separation curve where the crack propagation ends (see Figure 2.7).

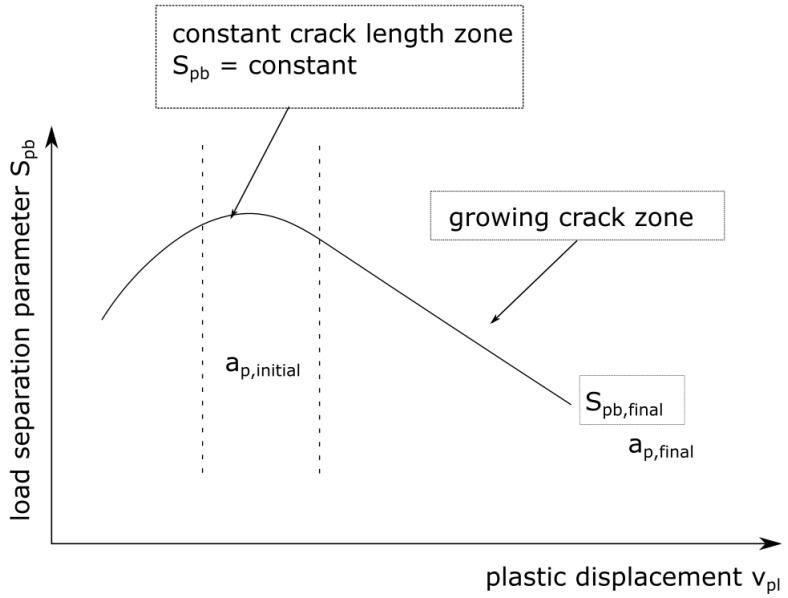

Figure 2.7.: *Characterization of the parameter m at the end of region II where the crack length in the sharp notched specimen a_p is known according to [35]*

In this case the starting point of the stable crack growth a_p is taken to calculate the exponent m. At this point the values of notch lengths are well known for sharp notched and blunt notched specimens. To determine the starting point of the stable crack growth from the load separation method a specific criterion, as described below, has been utilized [11].

First of all the maximum value of the load separation parameter $S_{pb,max}$ has been identified and 0.01 has been subtracted of this value and set as initiation point. The value of 0.01 was determined by Wainstein [35] and includes uncertainties within the crack growth initiation.

With the help of the calculated exponent m it is possible to calculate the crack length a_p as:

$$a_p = a_b \left(\frac{P_p}{P_b} \right)^{1/m} = a_b \left(S_{pb} \right)^{1/m} \tag{2.9}$$

Hence, the load separation parameter S_{pb} is directly related to the crack growth a_p in the sharp notched specimen [11].

In a next step the J-Integral can be calculated using:

$$J_0 = \frac{\eta U}{B(W - a_0)} \tag{2.10}$$

where η is a geometry depended factor (η=2 for SENB specimen), U is the area under the load displacement curve (absorbed energy), B is the specimen thickness, W the specimen height and a_0 the initial crack length of the sharp notched specimen. In the same way as discussed for the multi specimen method the absorbed energy U has to be corrected with the indentation correction. Finally the J-Integral has to be corrected for the amount of crack extension Δa where

$$\Delta a = a_0 - a_p \tag{2.11}$$

and the J-Integral can be written as:

$$J = J_0 \left[1 - \frac{(0{,}75\eta - 1)\Delta a}{W - a_0} \right]. \tag{2.12}$$

At the end it is possible to construct the crack resistance curve (J-Integral depending on the crack growth Δa) [11].

2.3.4. Influence of the chosen elastic compliance value

The influence of the chosen elastic compliance value on the determination of the J-R-curve via the load separation method was a major part of this work. In general the

elastic compliance value C is determined at the beginning of the load-displacement record of the tested specimens (see Figure 2.8).

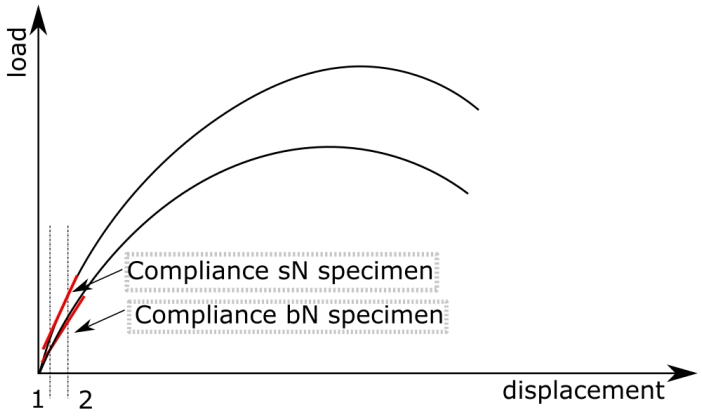

Figure 2.8.: *Determination of the elastic compliance value for sharp notched and blunt notched load-displacement records.*

In this work the elastic compliance C is determined between two different displacement values v (value 1 and value 2 in Figure 2.8). The first elastic compliance was determined between 0.1 mm and 0.2 mm displacement and the second elastic compliance value between 0.05 mm and 0.1 mm displacement. This variation was done for sharp notched sN and blunt notched bN specimens. This ends up in three different versions of load-displacement records and additionally three versions of load separation curves and J-R-curves. This variations has been examined, since it is not always easy to determine the exact elastic region for bend tests. Due to setting of specimen and the machine, this area can be shrouded. In normal bend-tests this is rectified by applying a certain pre-load and excluding this data from the test. However, due to the fact that even very low pre-loads can already induce plasticity around a sharp notch tip this data should not be excluded from the energy balance.

2.3.5. Determination of a parameter to indicate the crack advancement

The load separation method offers the opportunity to determine the parameter m_s in the region of stable crack growth (region III in Figure 2.7) where usually a linear trend of the load separation curve is determined. In general the parameter m_s is evaluated from the normalized separation parameter curve R_s, which is defined as:

$$R_s(v_{pl}) = \frac{S_{pb}(v_{pl})}{S_{pb,plateau}} \tag{2.13}$$

where S_{pb} is the load separation parameter curve and $S_{pb,plateau}$ the maximum value of the same curve (plateau in region II see Figure 2.7). In a next step it is possible to determine the parameter m_s:

$$m_s = -\frac{dR_s}{dv_{pl}}\bigg|_{v_{pl}>v_{pl,plateau}} \tag{2.14}$$

as the opposite of the slope of the normalized separation parameter R_s in region III of stable crack growth. The parameter m_s indicates the crack advancement produced per unit of plastic displacement v_{pl} and is similar for same materials. Hence, it is possible to use the parameter m_s as a classification of fracture propagation process in the plastic region [4].

3. Results

3.1. Multi specimen approach

The multi specimen approach was used to characterize the non linear elastic plastic fracture mechanics by the construction of the J-R-curve for PP-H, PP-R and PP-B. In the following chapters the results and the path to determine the J-R-curve with the help of the multi specimen method are described. It was challenging to construct a J-R-curve for various sorts of Polypropylene at room temperature, because of the extremly tough material behaviour of the tested Polypropylene specimens. Thus, the results should gain insight into the difficulties within the evaluation of the non linear elastic plastic material behaviour. In general it is typical to calculate the data points of the J-R-curve and in a next step reduce the determined data points in order to fit a power law function for the crack resistance curve. In this chapter all determined data points within the multi specimen method are presented and the reduced fitted J-R curves are shown in the comparison chapter. The relativ low maximum Δa values in the corresponding evaluations of the J-R curve are partly due to the plane sided specimen without side grooves. The stress state on the surfaces induce rather large plastic zones early on, which decreases the possibile amount of stable crack growth significantly 3.3 [36, 37].

3.1.1. Multi specimen approach using PP-H

In a first step, the fracture surface of Polypropylene-H (PP-H) after the bending tests is analysed in order to gain detailed information about the fracture process and to

characterize the produced crack length Δa. As discussed in the theoretical background the measurement of the crack length is a major part in the reconstruction of the fracture process. Figure 3.1 presents an overview of the crack surface of PP-H and some detailed pictures of characteristic regions during a fracture process with a higher magnification. As shown in Figure 3.1 there were three different regions detected. The beginning of fracture is characterized by the blunting process. This is shown on the overview with a red mark and in the detailed pictures with the red frame. This region is characterized by stretched filaments oriented in the direction of crack propagation. The blunting region is followed by stable crack growth (green mark in the overview and green frame) with a typical stress-whitened region. The blue marked region shows also a stress whitened zone but with a detailed look at the blue framed picture, the fracture surface is typical for a crack induced under cooling with liquid nitrogen. This last region is typical for plastic deformation mechanisms like crazing but there is no crack propagation detected. It is possible to define the area of stable crack growth until the end of the green marked region. In general, the whole fracture process is strongly influenced by the applied sharpening technique which directly influences the ratio of the plastic zones according to [11, 36, 37, 38, 39, 40, 41, 42].

After the determination of the crack growth Δa during testing, it is possible to calculate the J-Integral and construct the crack-resistance curve for every specimen of PP-H as shown in Figure 3.2. It is quite difficult to identify the area of stable crack growth Δa for every tested specimen, hence the determined data scatters significantly. Figure 3.2 represents the two determined J-R-curves (Multi 1, Multi 2) with the help of the multi specimen approach for PP-H. The curve Multi 1 represents the first version of the characterized crack resistance curve without a lot of knowledge about the area of stable crack growth and the exact crack propagation Δa. In this first version of the J-R-curve (Multi 1) the crack propagation Δa on the fracture surface of the tested specimens was defined a bit too high and it ends up in a lower slope of the J-Integral. For the second curve (represented by Multi 2) it was possible to correct the crack

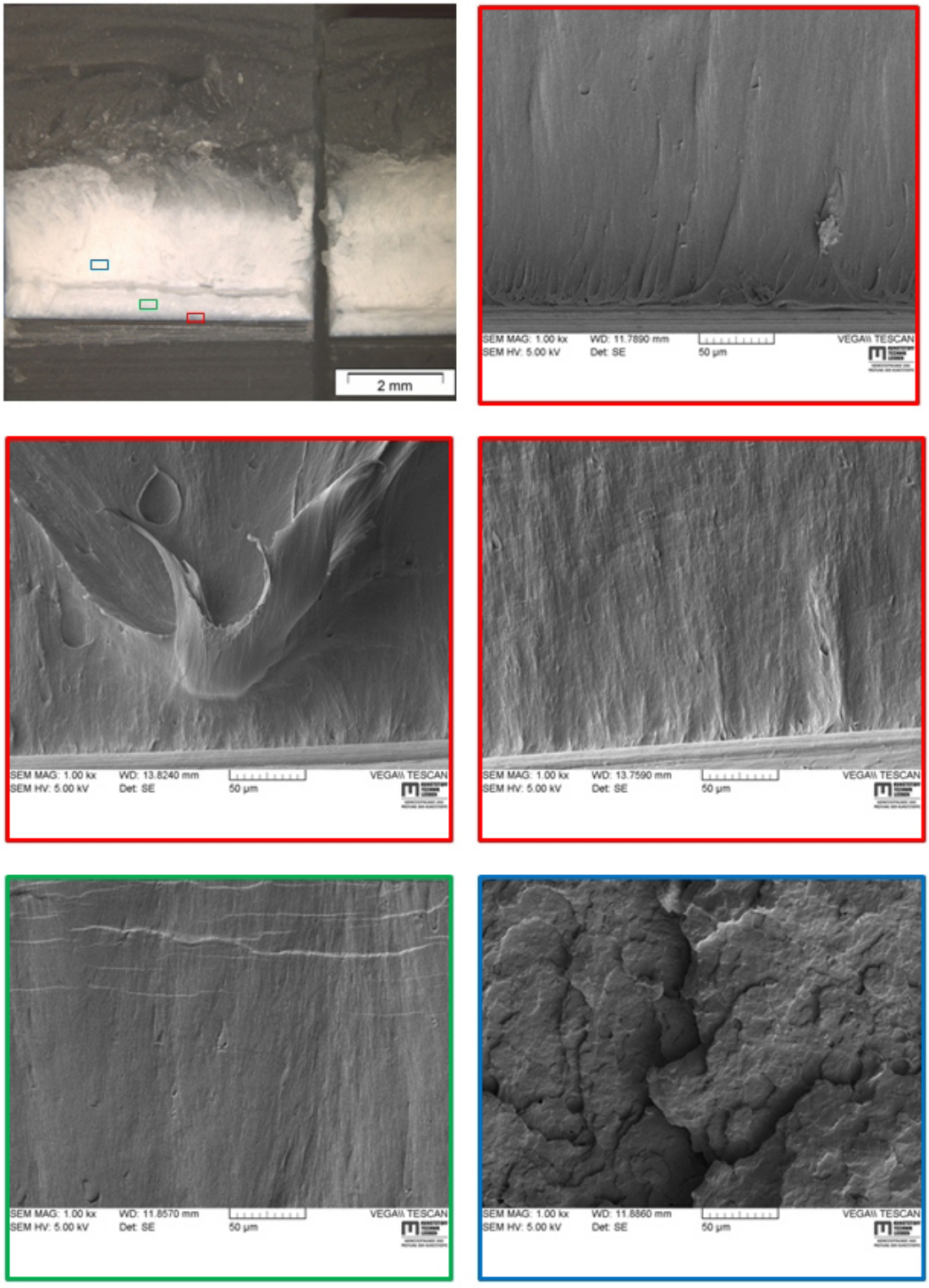

Figure 3.1.: *Fracture surface analysis of PP-H using light microscopy and SEM at a magnification of 1000x to characterize different crack zones: blunting zone (red), stable crack growth (green) and fracture caused by liquid nitrogen (blue).*

growth Δa to lower values and a new crack resistance curve was determined. This correction was possible after detailed analysis of many fracture surfaces of PP-H.

The characterized values of the J-Integral start at 5 kJ/m^2 and the maximum is around 45 kJ/m^2. The measured crack lengths Δa show values between 0 mm and 4 mm. The resulting J-R curve for PP-H is in a similar range compared to literature [43].

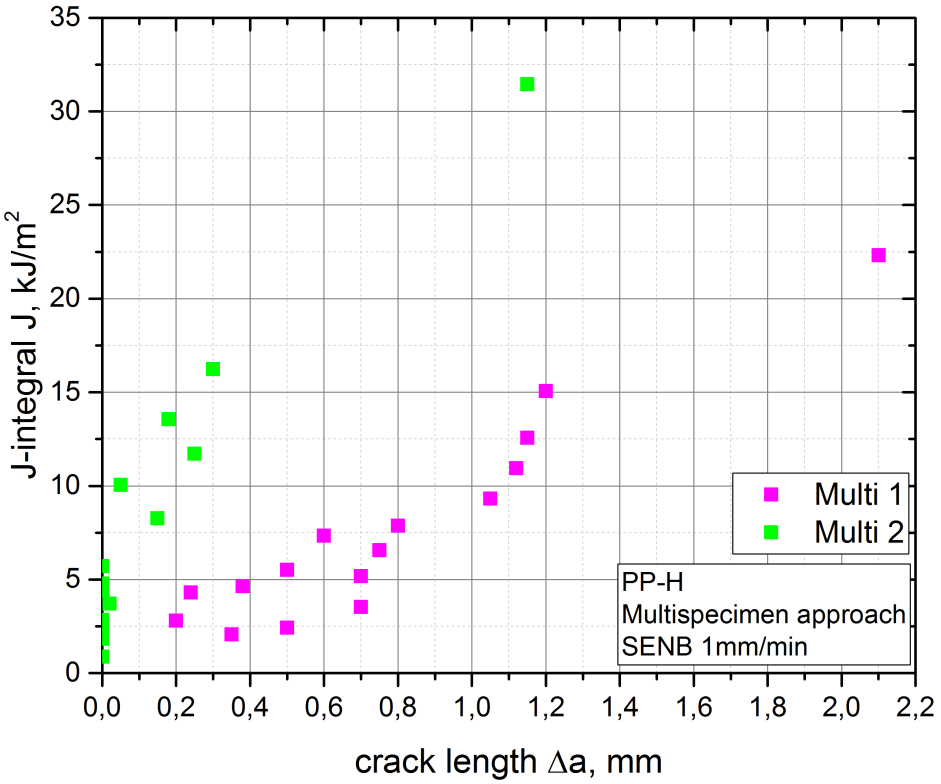

Figure 3.2.: *J-Integral depending on the crack length determined by the multi specimen approach for PP-H.*

3.1.2. Multi specimen approach using PP-R

In a next step the crack resistance curve for Polypropylene-R (PP-R) was determined with the multi specimen approach. In the same way as discussed for PP-H, the crack surface of PP-R was investigated in detail. Figure 3.3 represents an overview of the crack surface and some detailed pictures with a higher magnification to identify the

different regions in a crack propagation process as previously discussed. The blunting region is highlighted in red and shown in detail by the pictures with the red frame. The blunting is characterized by small formations of fibrils in the direction of crack propagation. This fibrils can be seen in all three figures of the blunting process (red frame). Afterwards stable crack growth is identified and marked green. The area of stable crack growth is flat and straight and, as seen on the overview picture, relatively equal and symmetrically on the fracture surface. Additionally, there is also a stress whitened zone (marked blue) in front of the stable crack growth. This stress whitened zone which is broken after imersion in liquid nitrogen and hence not associated with crack growth during the testing itself. Now it is possible to define the stable crack growth for PP-R which ends with the green marked region [11, 37, 36, 38, 40, 41].

After characterizing the crack lengths Δa for all specimens it is possible to determine the crack resistance curve of PP-R by the use of the multi specimen method (Figure 3.4). Similarly to PP-H, the characterization of the fracture surface of PP-R is not always clear, as is shown in Figure 3.3. Figure 3.4 presents two curves to show the influence of the identified crack lengths Δa. In the first version of the crack resistance curve (Multi 1) the crack front was assessed a bit too high and ended up in a lower slope (Figure 3.2). At the second version of the crack resistance curve (Multi 2) the crack length Δa was corrected according to SEM findings and a new J-R curve (J-Integral depending on the crack length Δa) was calculated for PP-R.

The J-R curve of PP-R shows values of the J-Integral around 5 kJ/m^2 to 20 kJ/m^2 at the beginning of the crack propagation. At the maximum value of characterized crack length Δa specimens reache a value around 45 kJ/m^2. The determined values of the crack resistance curve of PP-R are lower at the beginning compared to the calculated values of the J-R curve of PP-H. However, they show a stronger increase compared to PP-H. This is also proposed in literature [43] and can be explained by a combination of higher yield phenomena in the process zone and a higher COD (Crack opening displacement which is related to deformation processes) for PP-R.

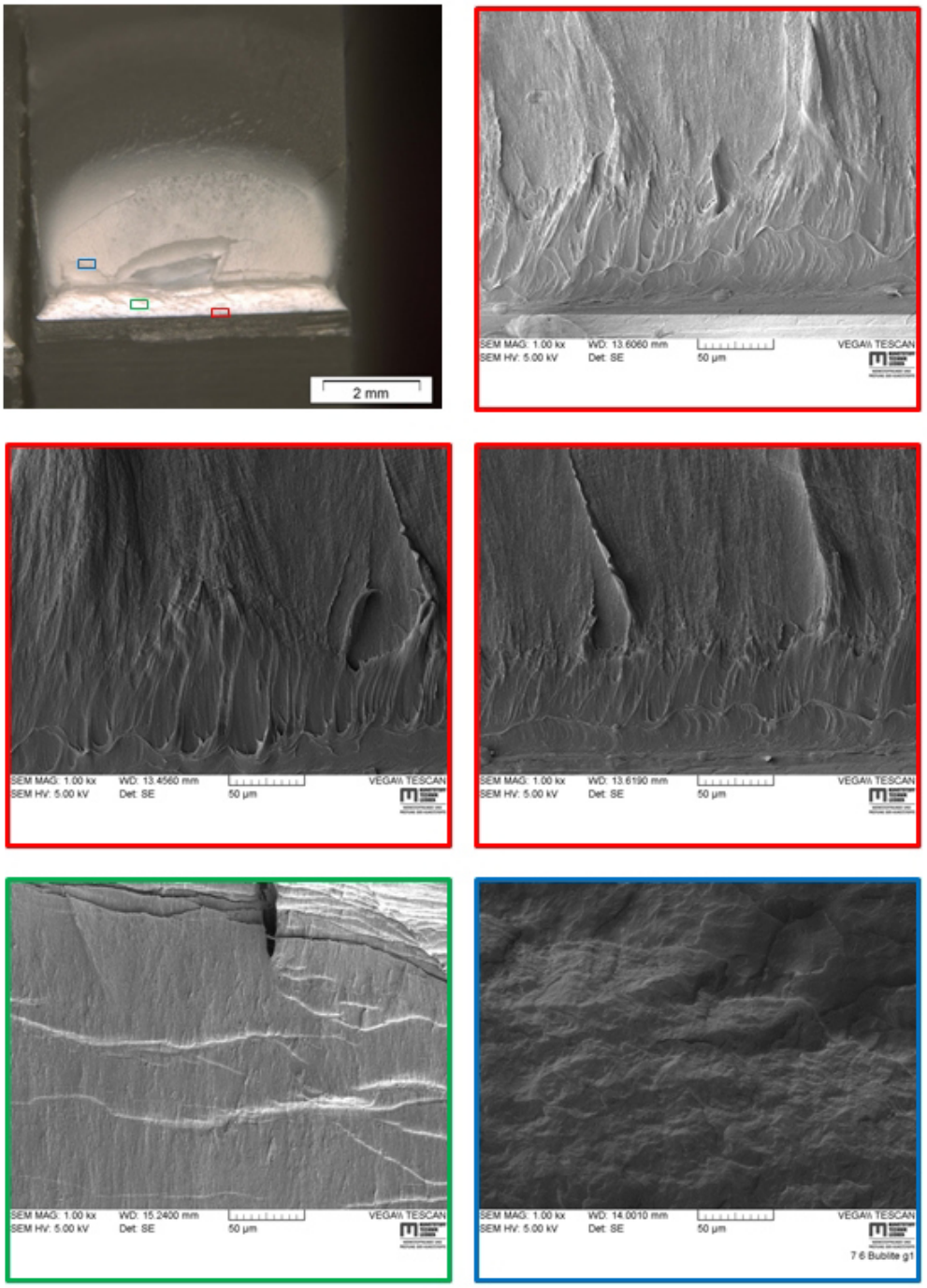

Figure 3.3.: *Fracture surface analysis of PP-R using light microscopy and SEM at a magnification of 1000x to characterize different crack zones: blunting zone (red), stable crack growth (green) and fracture caused by liquid nitrogen (blue).*

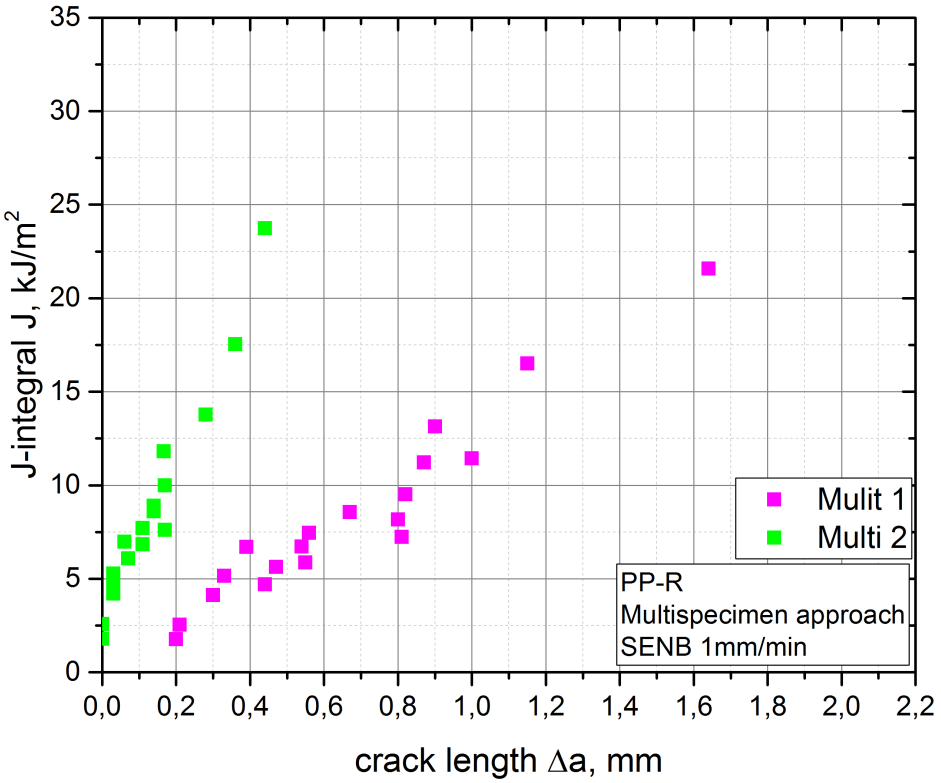

Figure 3.4.: *J-Integral depending on the crack length determined by the multi specimen approach for PP-R.*

3.1.3. Multi specimen approach using PP-B

Finally the fracture surface of Polypropylene-B (PP-B) was inspected in detail. Figure 3.5 shows an overview picture of the crack surface of PP-B and some detailed pictures with a higher magnification of the different crack zones during the fracture process. The first region detected on the fracture surface of PP-B is typical for blunting (red marked zone and red framed pictures). Additionally, there are some short fibrils detected in direction of the fracture process. The blunting process differs between all three characterized materials but the formation in the direction of crack propagation is detected on all specimens. Afterwards, stable crack growth is detected on the fracture surface and marked green. The area of stable crack growth is flat and straight with

less formations in the direction of crack propagation. The end of the stable crack growth and the beginning of the stress whitened zone is shown in the blue marked picture. The flat surface of stable crack growth ends up showing a completely different surface structure. The area of plastic deformation looks completly different to the blunting region and the region of stable crack growth and is broken up with liquid nitrogen [11, 37, 38, 40, 37, 41].

After identifying the area of stable crack growth, it is possible to calculate the J-Integral. In the same way as for PP-H and PP-R the J-R-curve was constructed for PP-B (see Figure 3.6). The determination of stable crack growth of the tested PP-B specimens was also not clear in the beginning and hence Figure 3.6 again represents the construction of the J-R-curve. In comparison to the tested specimens of PP-H and PP-R there were less specimens of PP-B indicating a clear area of stable crack growth. The points of Multi 1 present the measured stable crack growth and the calculated J-Integral of the first version. In the second version of the crack resistance curve (Multi 2), it was possible to correct the detected crack length of stable crack growth but in comparison to the other tested materials the PP-B specimens show a much more complex fracture mechanism.

The determined J-R-curve for PP-B shows values of the J-Integral between 5 kJ/m^2 at the beginning of the crack propagation and 25 kJ/m^2 around 0.35 mm crack length Δa. The values of the determined J-R curve of PP-B are lower than the calculated values for PP-H and PP-R. In comparison to literature, the calculated J-R-curve of PP-B shows similar results [42, 43].

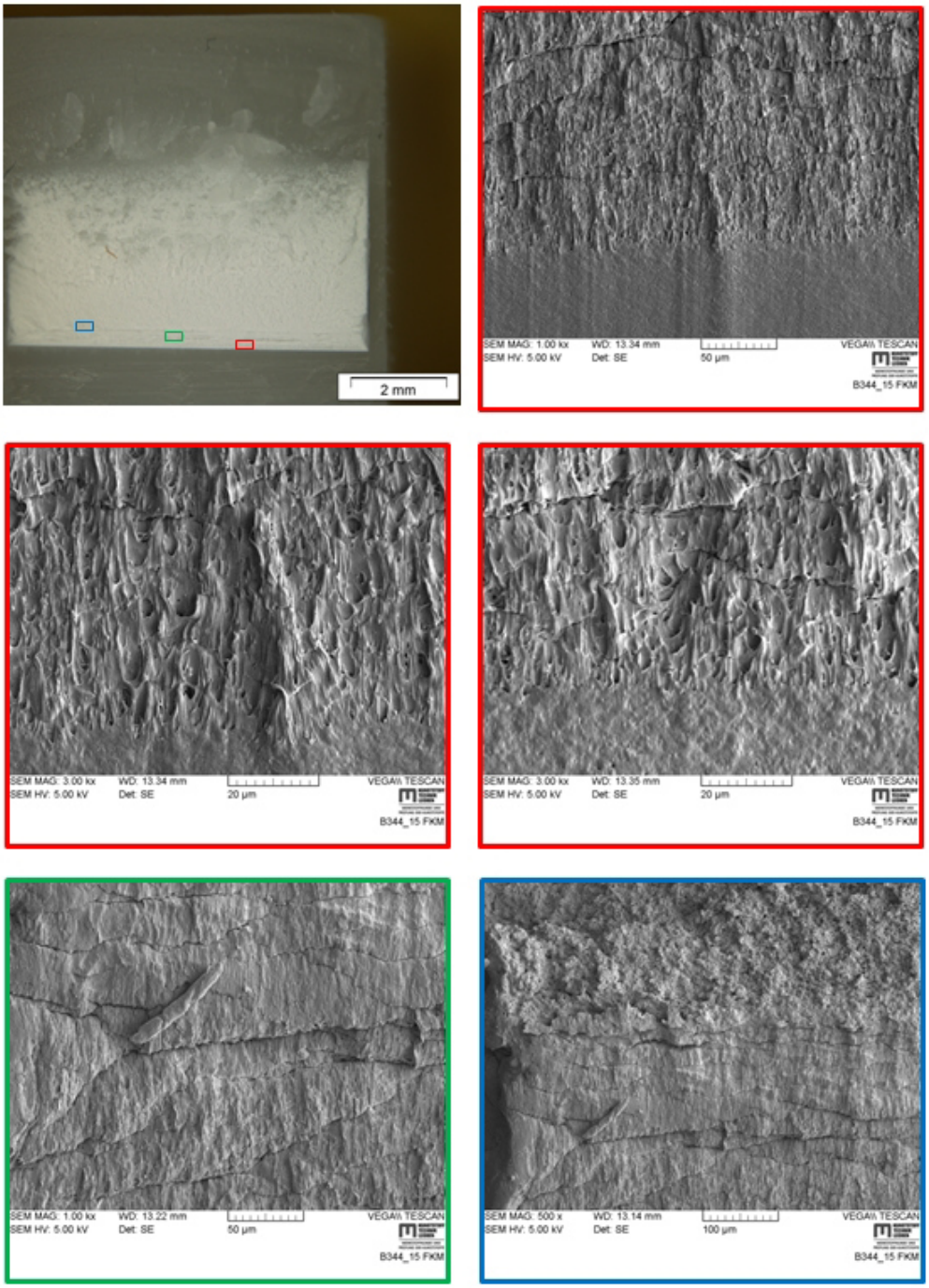

Figure 3.5.: *Fracture surface analysis of PP-B using light microscopy and SEM at a magnification of 1000x to characterize different crack zones: blunting zone (red), stable crack growth (green) and fracture caused by liquid nitrogen (blue).*

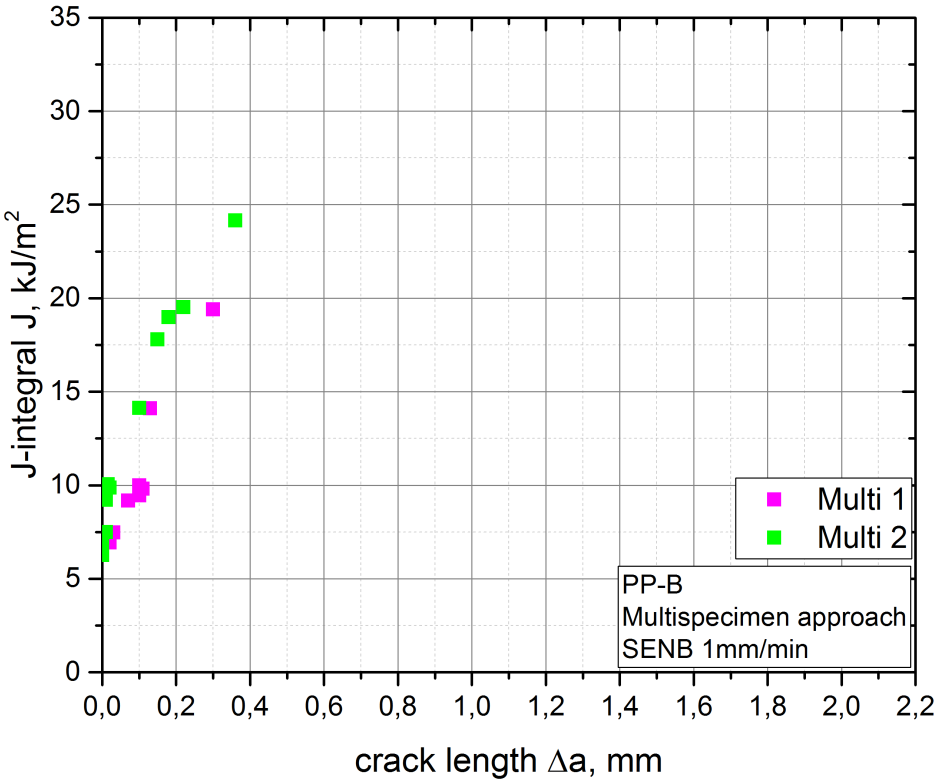

Figure 3.6.: *J-Integral depending on the crack length determinde by the multi speicmen approach for PP-B.*

The results of the shown J-R-curves via the multi specimen method are compared with the results of the load separation method in chapter 3.3.

3.2. Load separation Method

In this section, the application of the load separation method to characterize the crack resistance curve of PP-H, PP-R and PP-B is described. In a first step the crack surfaces of the tested specimens were characterized in detail to investigate the crack propagation Δa in the sharp notched specimen. Afterwards the load separation method is applied to characterize the crack resistance curve for all tested materials (J-R-curve). The big advantage of the load separation method is the determination of

the crack propagation Δa in the sharp notched specimen during testing with the help of the load separation parameter S_{pb}. Hence it is possible to reduce errors within the determination of the crack propagation Δa directly on the fracture surface. However, the load separation method itself has also a lot of influencing factors and correct application may proove challenging. The following chapters should also provide a view on the difficulties within this method [11, 34].

3.2.1. Load separation method for PP-H

The crack surface of the sharp notched sN and blunt notched bN specimens of PP-H are shown in Figure 3.7. To achieve representative results via the load separation method, a region of stable crack growth in the sharp notched specimens is required. In this case only one tested sample show stable crack growth (PP-H sN1, Figure 3.7). The other two sharp notched samples (PP-H sN2 and PP-H sN3, Figure 3.7) did not fullfill the requirements for the load separation method.

The blunt notched specimen acts as a reference for the sharp notched specimen and is of major importance for the application of the load separation method. For the blunt notched specimens, it is important that no crack propagation is detected on the fracture surface. Of all the tested blunt notched samples, only PP-H bN1 (Figure 3.7) shows no crack propagation and is admitted for the load separation method. The other two samples (PP-H bN2 and PP-H bN3, Figure 3.7) show crack propagation. Therefore, they are not useable for the characterization [11].

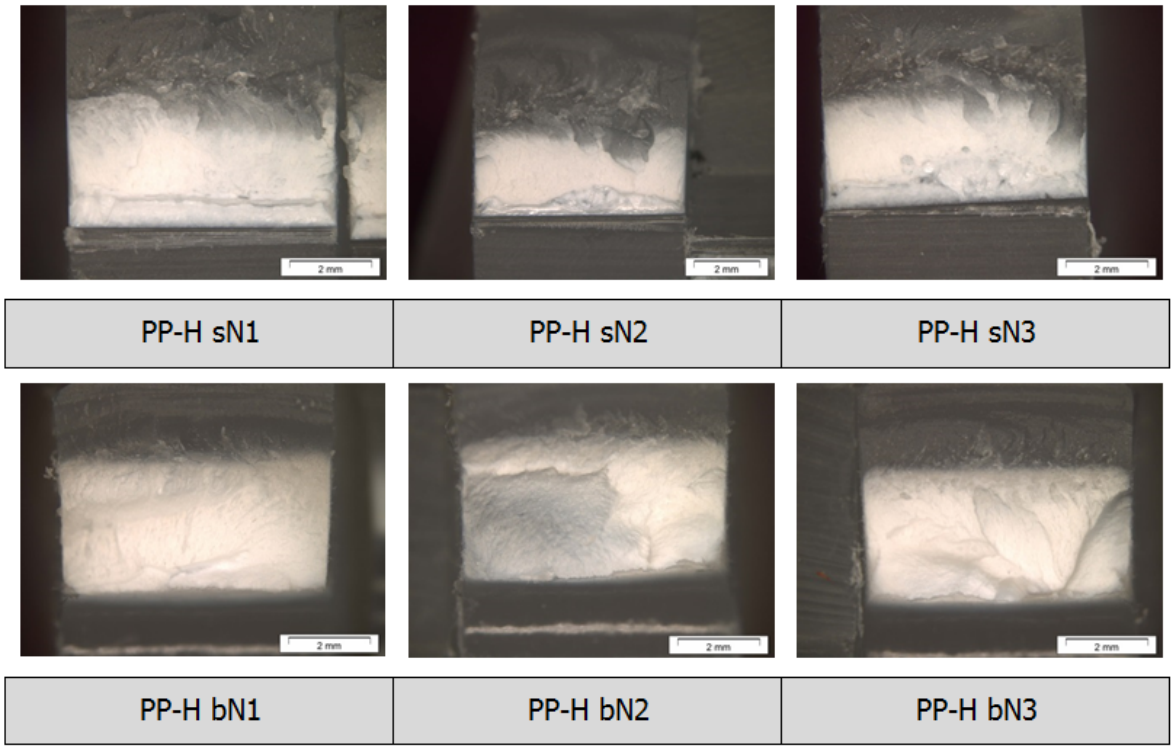

Figure 3.7.: *Fracture surface analysis with the light microscopy of sharp notched (sN) and blunt notched (bN) specimens of PP-H.*

After a detailed analysis of the crack surface, the load separation method is applied to the chosen sharp notched and blunt notched specimens to construct a crack resistance curve. First, the load F versus plastic deformation $v_{plastic}$ curves for different elastic compliance values were calculated (Figure 3.8). For better understanding two different regions where the elastic compliance of the specimen is determined were used to subtract the elastic part from the measured displacement v. The first elastic compliance was determined in the region between 0.1 mm and 0.2 mm displacement v and the second elastic compliance was investigated between 0.05 mm and 0.1 mm. The two different elastic compliance values were applied to sharp notched specimens and blunt notched specimens to determine the plastic deformation $v_{plastic}$. Hence, it is possible to construct three different versions of load P depending on the plastic displacement $v_{plastic}$ curves for PP-H sharp notched specimens and PP-H blunt notched specimens (ver1, ver2 and ver3). Especially at low plastic deformations $v_{plastic}$ the

influence of the subtracted elastic compliance results in differing load P levels at corresponding plastic displacement $v_{plastic}$. The calculated elastic compliance is lower (and thereby the results of the plastic deformation are higher) when it is determined in a lower range of measured displacement (0.05 mm to 0.1 mm). Therefore the calculated sN ver3 and the bN ver2 (both with the lower range to calculate the elastic compliance) end up at lower load levels at the same plastic displacement. But at higher plastic deformations values, they are nearly the same. Because the part of plastic deformations in the tested specimens gets more significant at higher displacements values during testing. Hence, the differences of the determined load P versus plastic deformation $v_{plastic}$ curves show nearly the same values at higher plastic deformation values. This is also discussed in literature [4] but only when the load separation parameter is normalized as discussed in chapter 3.4.

Generally the load measured at the sharp notched sN and of the blunt notched bN specimens increase monotonically with the plastic deformation $v_{plastic}$. The sharp notched specimens also show a slight relaxation of the load P at a higher plastic displacement $v_{plastic}$. The mentioned relaxation of the load (decrease of the load after the maximum value) is connected to the idea that cracks initiate differently depending on the degree of crystallinity. According to literature [11] a lower relaxation of the load P with an increasing cristallinity is expected. The morphology of the tested materials show formations of large spherulites most likely in α-modification [33]. Hence, the differences concerning the relaxation of the load P within the three types of Polypropylene can be connected to the degree of cristallinity.

In this case the measured curves for the application of the load separation method are strongly influenced by the testing of the blunt notched specimen. The measured blunt notched specimens limited the maximum available displacement v for the application of the load separation method also for the sharp notched specimens. When crack propagation is detected on the blunt notched specimen it is no longer possible to determine a crack resistance curve. In general the tested PP-H show the highest load values compared to the other materials (PP-R and PP-B) tested in this study [33].

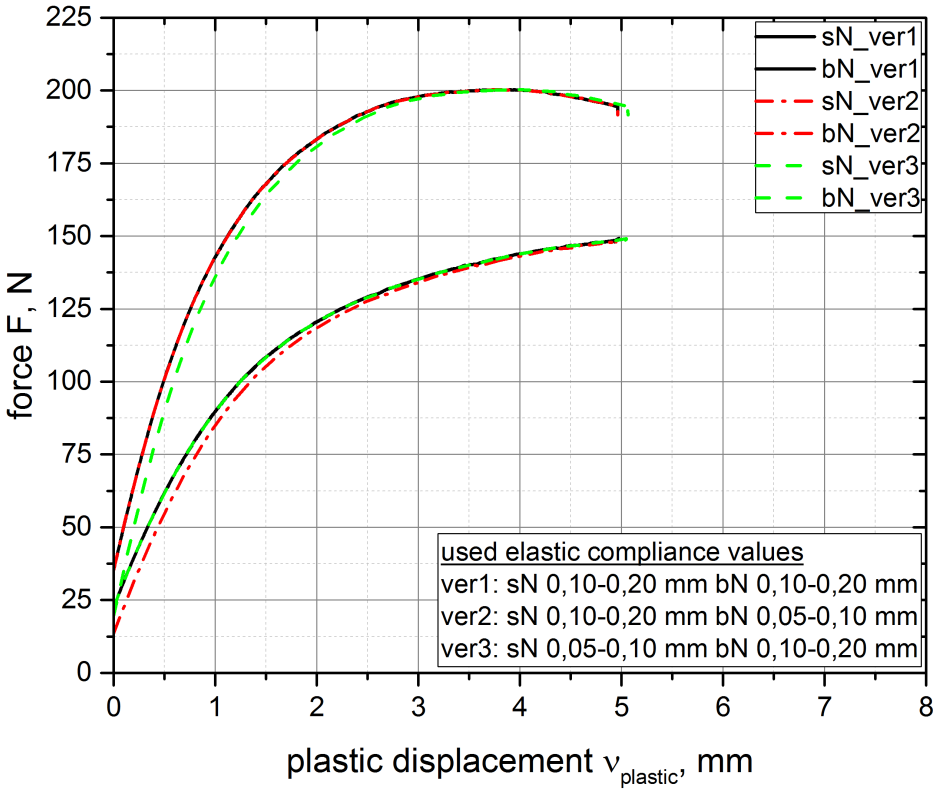

Figure 3.8.: *Load P depending on the plastic deformation $\nu_{plastic}$ for different elasitc compliance correction values for PP-H.*

With the help of the determined load P depending on the elastic compliance curves it is possible to construct the load separation parameter S_pb curve (Figure 3.9). There are major differences in the results of the load separation parameter S_pb curve depending on the plastic deformation $\nu_{plastic}$ for the different used elastic compliance values. All three load separtion curves show three typical regions. The first region I, the "unseparable" region at very low plastic displacement $\nu_{plastic}$, is characterized by a highly unstable S_{pb}. Hence, in region I, the separation principle is not valid. Followed by region II, the "plateau" region. This region is typical for the blunting process of the sharp notched specimen and shows nearly constant values of the load separation parameter. The last region (III), named "fracture propagation" region is typical for the fracture process in the sharp notched specimen and shows a decreasing load separa-

tion parameter S_{pb}. The determined load separation parameter curves differ at low plastic deformation $v_{plastic}$ values (region I) but end up in the same slope in region III for every version of chosen elastic compliance. The maximum values in region II of the three curves are different and the maxima occur at different values of plastic displacement $v_{plastic}$. The maximum of the load separation curve is necessary to identify the starting point of fracture propagation. In this case the occurred differences in region II of the load separation parameter curves definitely influences the determination of the crack resistance curve. But the same slope of the load separation curves in region III indicates a key role in the application of the load separation principle [4, 11].

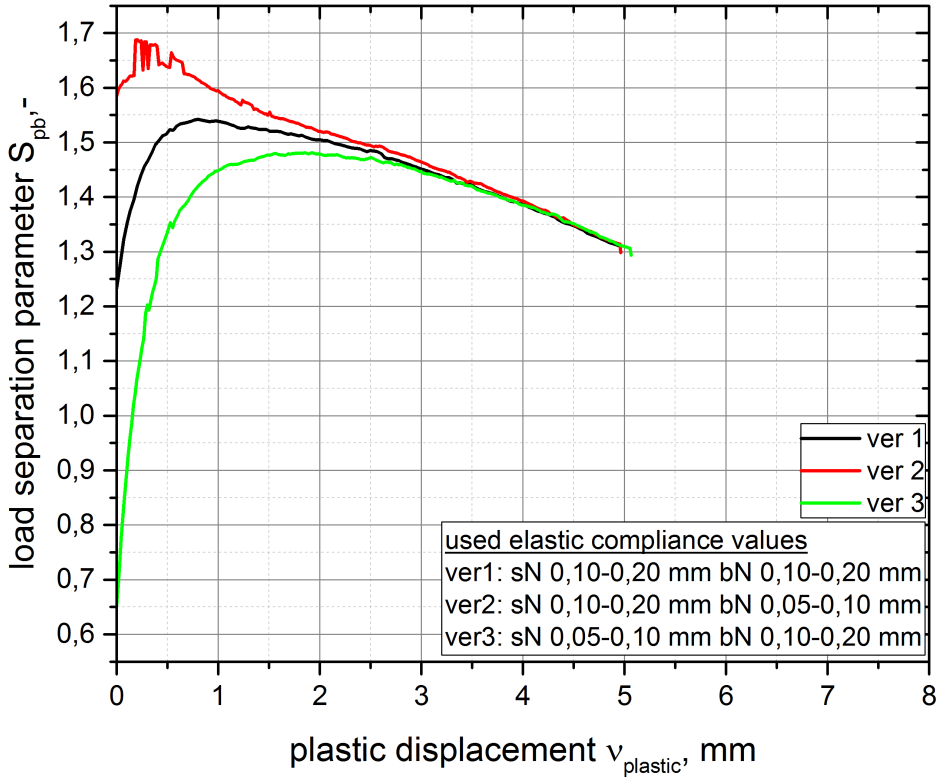

Figure 3.9.: *Load separation parameter S_{pb} depending on the plastic deformation $v_{plastic}$ for different used elastic compliance values for PP-H.*

Finally it is possible to determine the crack resistance curve for PP-H (J-Integral depending on the crack length Δa shown in Figure 3.10) for different used elastic

compliance values. The maximum J-Integral values are the same for all three versions of the used elastic compliance. But there are differences in the calculated amounts of crack length Δa.

The determination of the crack length Δa is connected with the chosen starting point of the load separation curve in region III. This staring point is influenced by the chosen elastic compliance and results in different amounts of crack length Δa. At this point it is important to refer the method of the "normalized separation parameter" according to [4]. There the load separation parameter S_{pb} gets normalized by its maximum and a parameter m_s, which characterizes the region III of the normalized load separation curve, is determined. But the result of this normalization method is no longer a crack resistance curve it is just a single parameter to rank different materials concerning their fracture behaviour. As a conclusion the chosen elastic compliance influences the maximum of the load separation parameter and in a next step the starting value of the J-Integral. Whereby the slope of all different load separation parameter curves is the same in region III. Additionally, the slope of the load separation curves in region III indicates a key role in the characterization of the J-Integral. In chapter 3.3 the results of the multi specimen method are compared with the results of the load separation method.

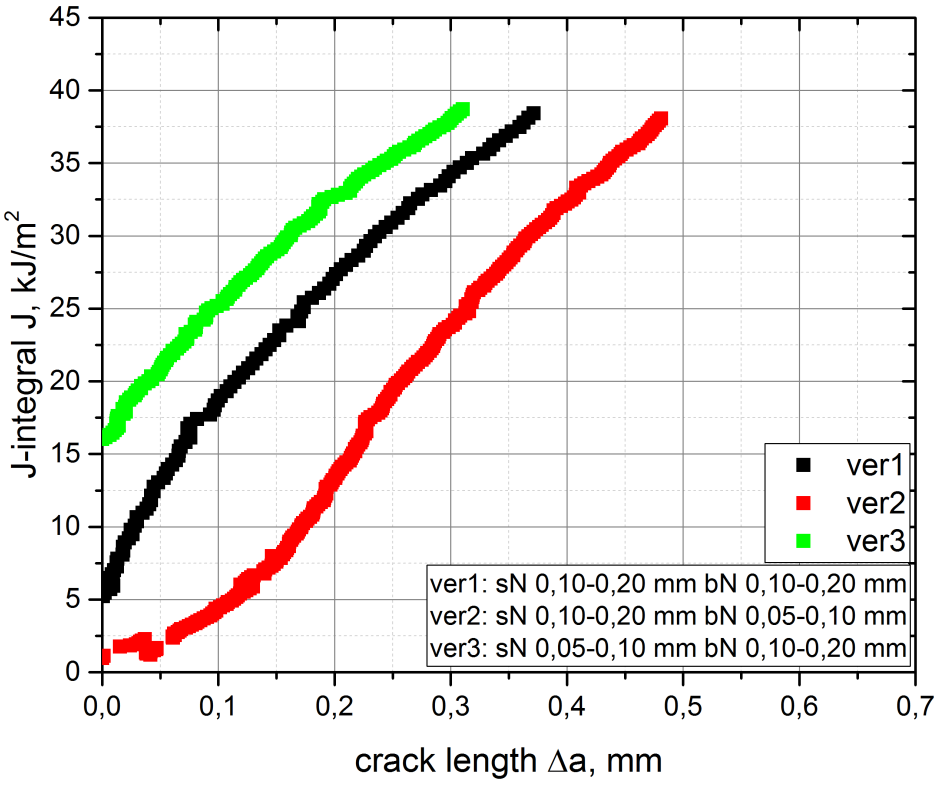

Figure 3.10.: *J-Integral depending on the crack length Δa for different used elastic compliance values for PP-H.*

3.2.2. Load separation method for PP-R

Additionally the load separation method was used to ascertain the crack resistance curve of PP-R. Figure 3.11 presents the fracture surface of sharp notched (sN) and blunt notched (bN) tested PP-R specimens. For the application of the load separation method only one tested sharp notched specimen fullfills the requirements of stable crack growth (PP-R sN1 see Figure 3.11).

Similar to the sharp notched specimens the blunt notched specimens have also preconditions for the use within the load separation method. There is no crack propagation allowed in the blunt notched specimens. In this case there are two tested

blunt notched specimens (PP-R bN1 and PP-R bN3, Figure 3.11) which are able to be used as reference for the sharp notched specimen [11].

After identification of the usable specimens it is possible to use the load separation method to construct a crack resistance curve J-R curve for PP-R.

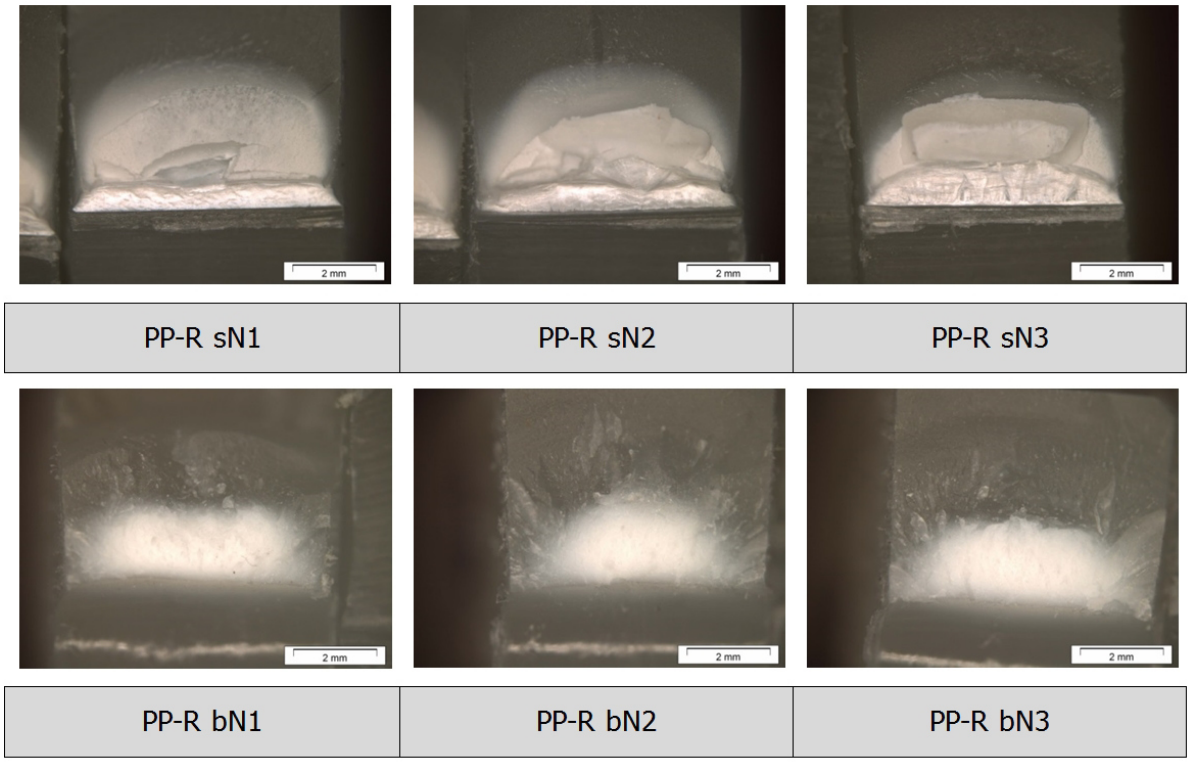

Figure 3.11.: *Fracture surface of sharp notched (sN) and blunt notched (bN) specimens of PP-R.*

Load separation method PP-R (sN1 with bN1)

At first, the load separation method was applied to the sharp notched specimen PP-R sN1 with the blunt notched specimen PP-R bN1 as reference. Figure 3.12 shows the load P depending on the plastic displacement $v_{plastic}$ for different used elastic compliance values. The different chosen elastic compliance values to determine the plastic displacement $v_{plastic}$ are the same as for PP-H. The first elastic compliance value was determined between 0.1 mm and 0.2 mm displacement and the second elastic compliance value between 0.05 mm and 0.1 mm. This ends up in three different versions of chosen elastic compliance values (ver1, ver2 and ver3) for PP-R (sN1 with

bN1). In the same way as for PP-H the determined elastic compliance value in the lower area (between 0.05 mm and 0.1 mm) ends up in a higher plastic displacement at the same amount of load P for sharp notched and blunt notched specimens, whereas all load curves end up in nearly the same range for sharp notched and blunt notched specimens with different chosen elastic compliance.

The curves of the sharp notched specimens increase monotonically and additionally show some relaxation of the load P after the maximum value which is related to the morphology of the material. The morphology of PP-R is additionally characterized as α-crystallization but also with a tendency to form crystallization in γ-modification. The crystallization in γ-modification causes a lower crystallization speed and hinders an overall crystallization according to literature [33]. Compared to the measured load P depending on the plastic deformation $v_{plastic}$ of PP-H the values of PP-R are in general lower and the maximum load is detected at higher plastic deformation values [11, 33].

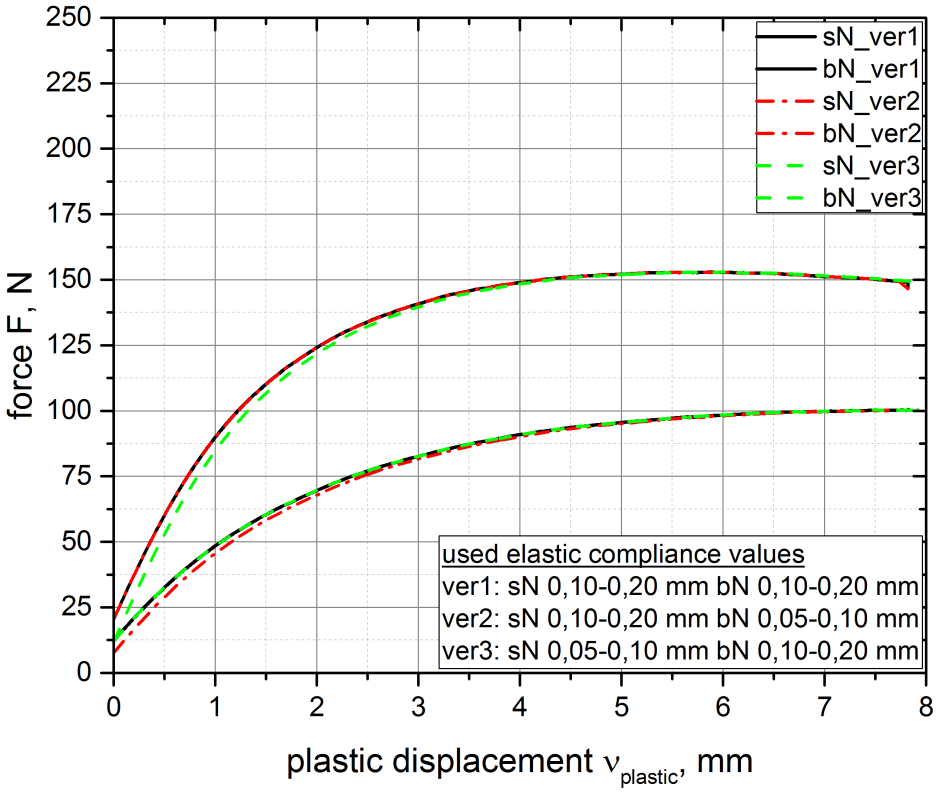

Figure 3.12.: *Load P depending on the plastic deformation $v_{plastic}$ for different elastic compliance correction values for PP-R (sN1 with bN1).*

With the determined load versus plastic displacement $v_{plastic}$ curves it is possible to construct the load separation parameter curve (Figure 3.13). In the same way as for PP-H the load separation parameter curve of PP-R (sN1 with bN1) shows a different behaviour in region I and region II but ends up in the same slope in region III for all different used elastic compliance values. Hence, the solpe in region III is an important parameter to characterize the non linear elastic material behaviour without any dependence to the chosen elastic compliance values [4].

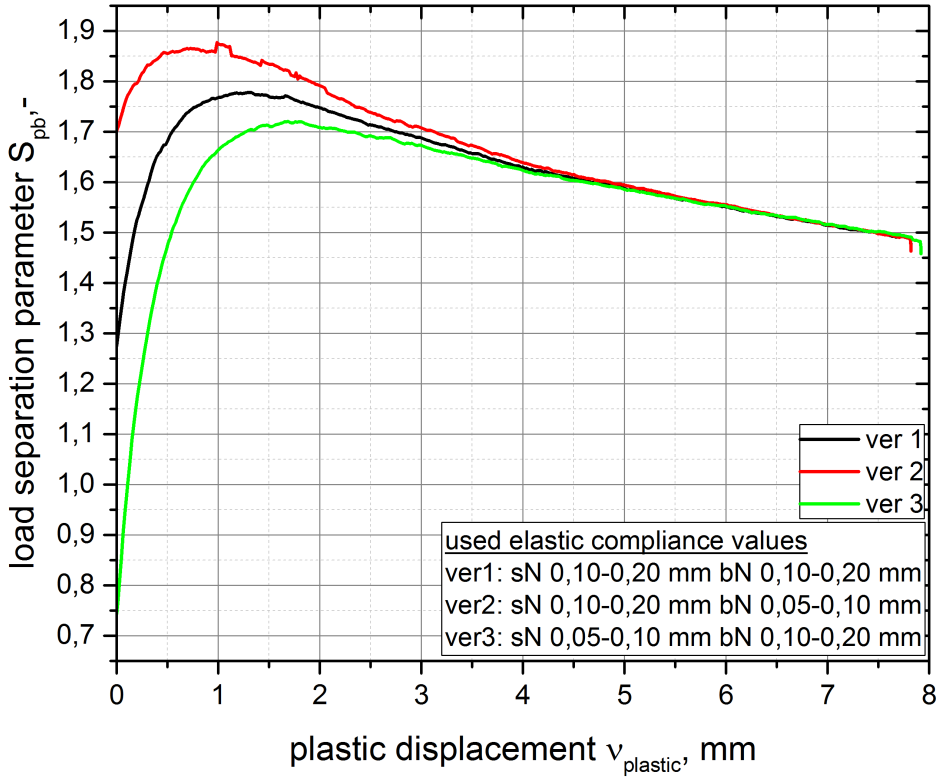

Figure 3.13.: *Load separation parameter S_{pb} depending on the plastic deformation $v_{plastic}$ for different used elastic compliance values for PP-R (sN1 with bN1).*

Now it is possible to calculate the crack resistance curve J-R-curve for PP-R (sN1 with bN1) determined with the help of the load separation principle. The calculated crack resistance curve for PP-R (sN1 with bN1) is presented in Figure 3.14. Additionally, the influence of the chosen elastic compliance values to the results of the crack resistance curve are shown. As mentioned in chapter 3.2.1, the maximum value of the load separation parameter has a major influence on the starting point of the J-R curve. As discussed before, the maximum value of the load separation parameter is in region II, and depends on the chosen elastic compliance. Therefore, it is a good opportunity to determine furthermore parameters to characterize the fracture behaviour which are independent of the chosen elastic compliance. As discussed before, the parameter m_s determined in region III of the load separation curve is an opportunity [4, 11].

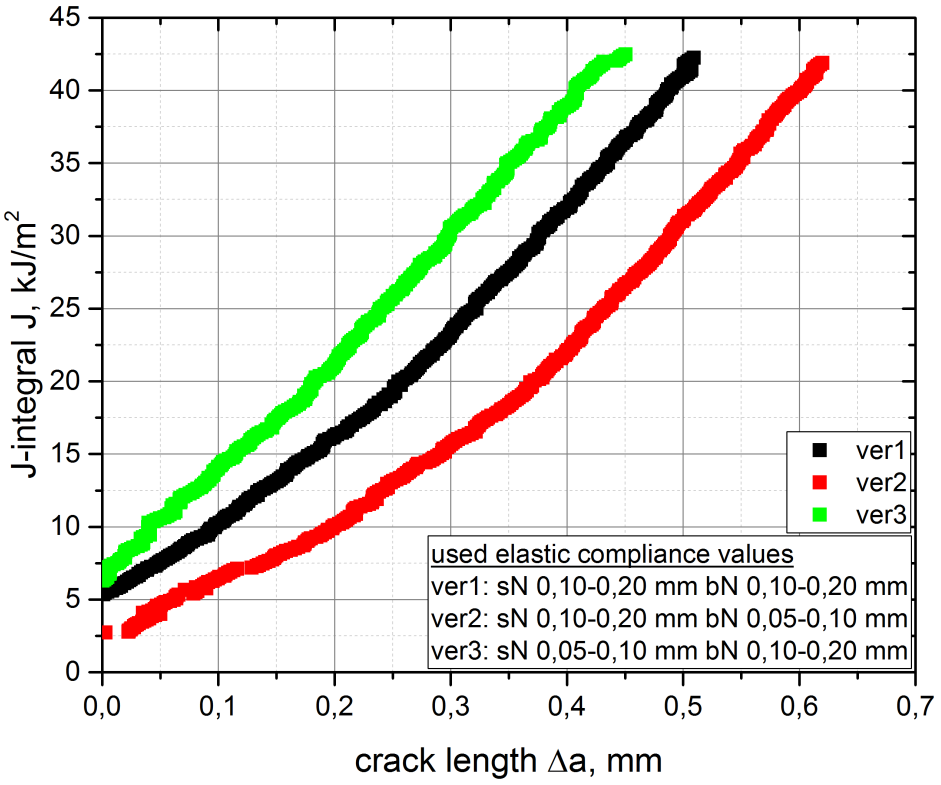

Figure 3.14.: *J-Integral depending on the crack length Δa for different used elastic compliance values for PP-R (sN1 with bN1).*

Load separation method PP-R (sN1 with bN3)

In this section the load separation method is applied to the specimens PP-R sN1 and PP-R bN3. First the load P depending on the plastic displacement $v_{plastic}$ with different used elastic compliance values are shown in Figure 3.15. In the same way as discussed before the two different used compliance values end up in three versions (ver1, ver2 and ver3) of the load versus the plastic displacement $v_{plastic}$ for PP-R (sN1 with bN3). The values of the determined load P of the blunt notched specimens PP-R bN1 and PP-R bN3 differ slightly, whereas PP-R bN3 shows a bit higher values of the load P. In general the measured load curves of PP-R show lower values compared to PP-H, which is to be expected, considering stiffness and yield stress of the materials [33].

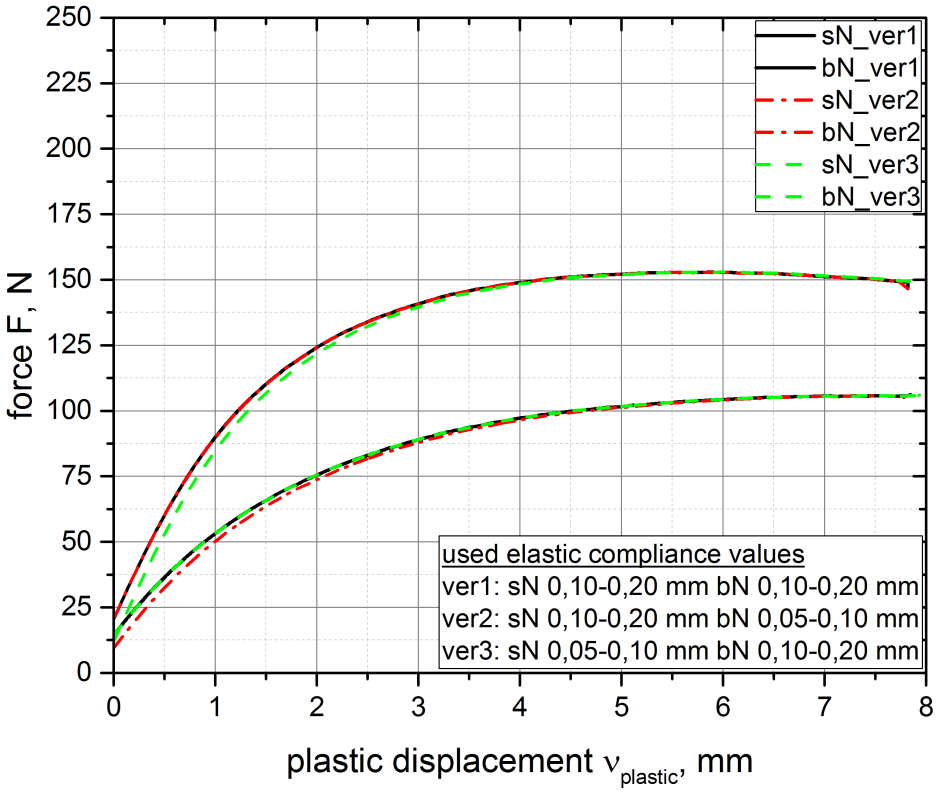

Figure 3.15.: *Load P depending on the displacement for for different elastic compliance correction values PP-R (sN1 with bN3).*

Now it is possible to calculate the load separation parameter curve for PP-R (sN1 and bN3) presented in Figure 3.16. In the same way as discussed before the load separation curves with different elastic compliance corrections end up in nearly the same slope in region III. Whereas, in region I and region II the curves show differences [11].

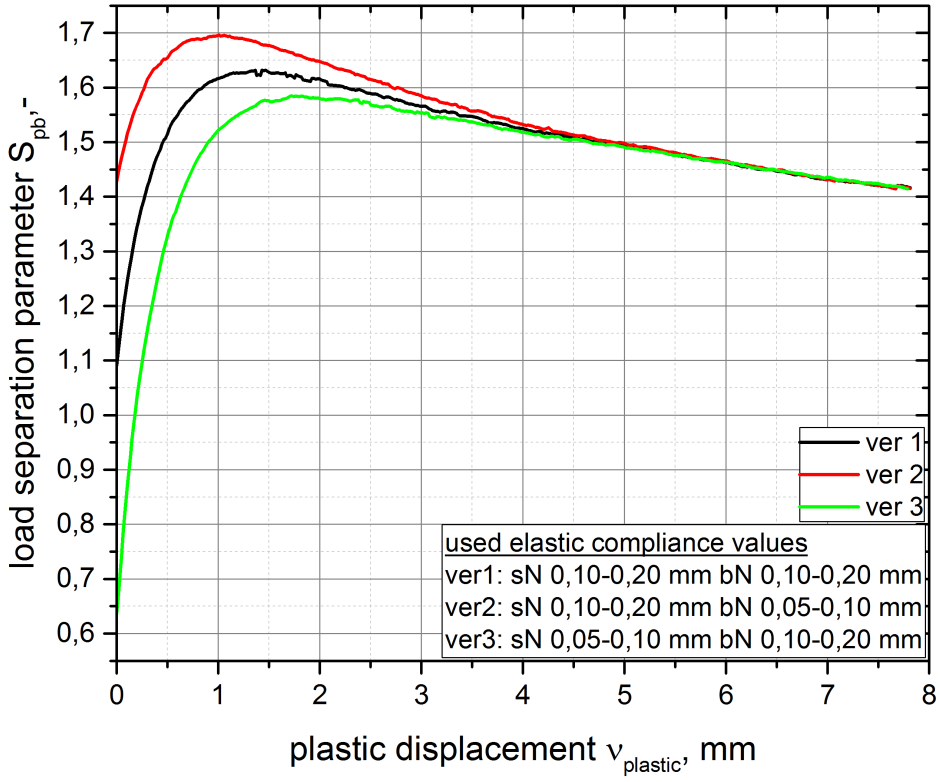

Figure 3.16.: *Load separation parameter S_{pb} depending on the plastic deformation $v_{plastic}$ for different used elastic compliance values for PP-R (sN1 with bN3).*

The determined crack resistance curve for PP-R (sN1 with bN3) from the load separation method is shown in Figure 3.17. The chosen elastic compliance value influences the crack resistance concerning the ordinate interception but the slope of all different J-R-curves is nearly the same. The starting point of the crack resistance curve is directly linked to the maximum value of the load separation point and its maximum value in region II, where the load separation parameter shows a strong dependence to the chosen elastic compliance value.

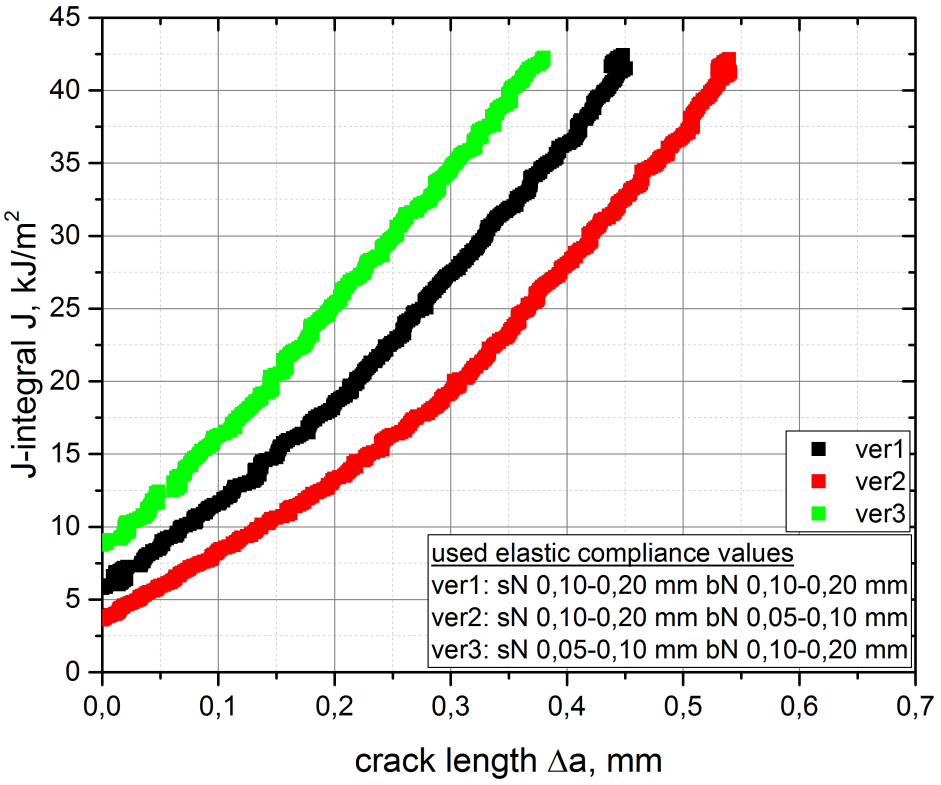

Figure 3.17.: *J-Integral depending on the crack length Δa for different used elastic compliance values for PP-R (sN1 with bN3).*

3.2.3. Load separation method for PP-B

The load separation principle is used to characterize the crack resistance curve (J-R curve) of PP-B. Similar to the discussed materials PP-H and PP-R, the influence of the used elastic compliance C to determine the plastic deformation $v_{plastic}$ is analysed in detail.

In a first step, the fracture surfaces of the tested sharp notched sN and blunt notched bN specimens are investigated and presented in Figure 3.18. For the correct use of the load separation principle the sN and the bN specimens have to full fill requirements. Whereas the sN specimen should show a clear stable crack growth, no crack growth should be detected in the bN specimens. In this case, both blunt notched

specimens of PP-B fullfill the requirements and are able to be used as reference for the characterization of the crack resistance curve of PP-B but only one sharp notched specimen of PP-B shows stable crack growth (PP-B sN4 see Figure 3.18).

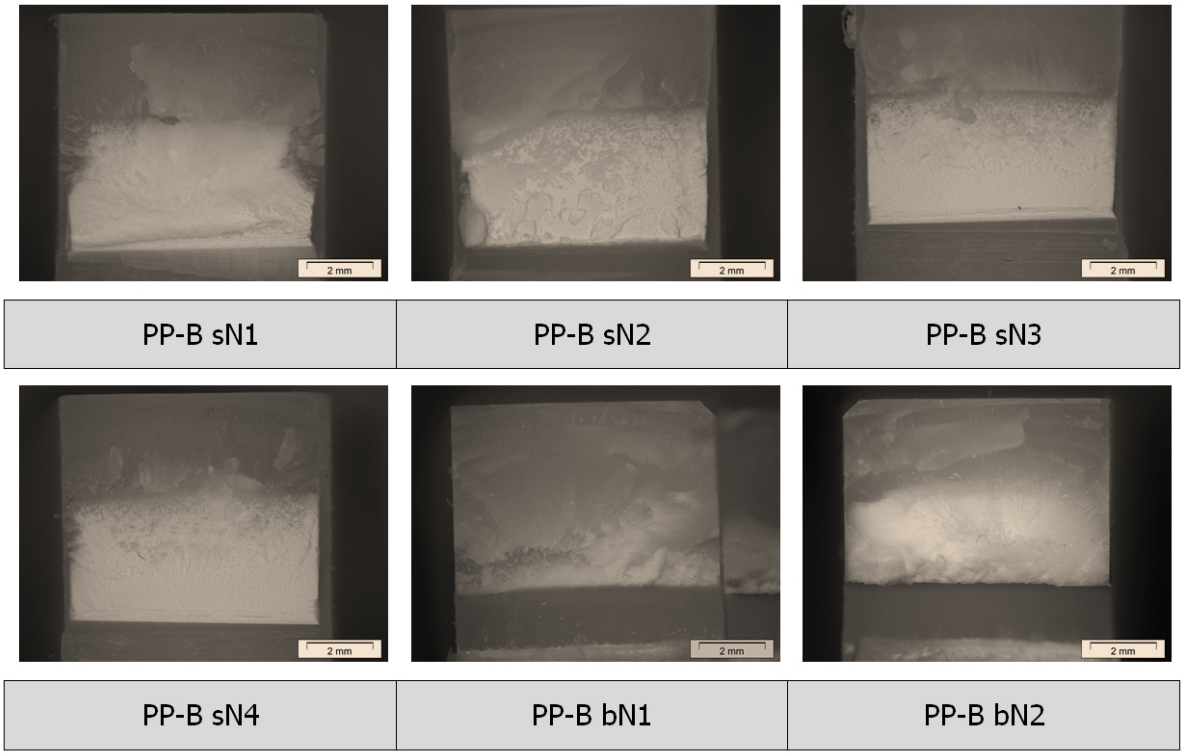

Figure 3.18.: *Fracture surface of sharp notched (sN) and blunt notched (bN) specimens of PP-B.*

With the chosen specimens PP-B sN4, PP-B bN1 and PP-B bN2, it is possible to determine the load separation parameter and in a next step to calculate the crack resistance curve of PP-B.

Load separation method PP-B (sN4 with bN1)

First of all the load P versus plastic deformation $v_{plastic}$ curves for PP-B (sN4 with bN1) is presented in Figure 3.19. As discussed before, the value of the chosen elastic compliance to determine the plastic deformation $v_{plastic}$ varies between 0.1 mm and 0.2 mm and the second time between 0.05 mm and 0.1 mm for bN and sN specimens. This ends up in three different load P depending on the plastic deformation $v_{plastic}$ curves

(ver1, ver2 and ver3). The influence of the chosen elastic compliance is discussed like for tested PP-H and PP-R samples on the whole application of the load separation method to calculate the crack resistance curve for PP-B. As mentioned above a characterization of the elastic compliance in a lower value of displacement (0.05 mm to 0.1 mm) ends up in higher plastic displacements compared to the higher values of calculated elastic compliance (0.1 mm to 0.2 mm) at the same load levels. Measured load levels of sharp notched and blunt notched PP-B samples are slightly higher in comparison with the presented load levels of PP-R but clearly lower than the measured load levels of PP-H. This material behaviour was also observed in literature [33].

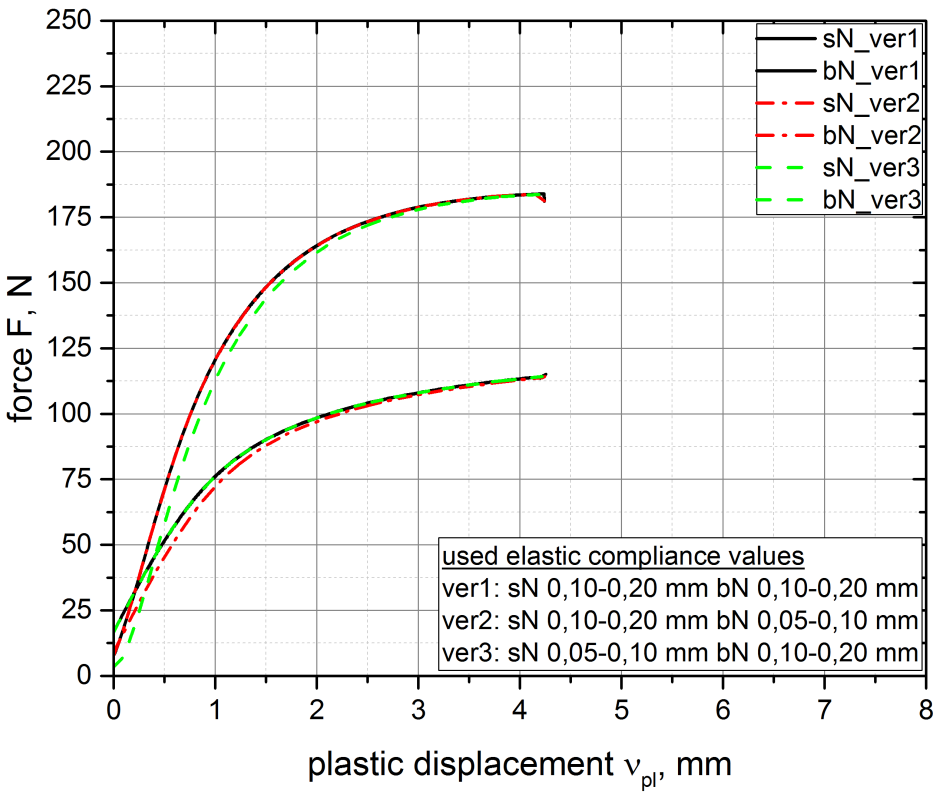

Figure 3.19.: *Load P depending on the plastic displacement $v_{plastic}$ for different elastic compliance correction values of PP-B (sN4 with bN1).*

Figure 3.20 presents the calculated load separation curves for PP-B (sN4 with bN1) determined using different elastic compliance values. The load separation curves

show differences in region I and region II and while the maximum values are different, they end up in the same slope in region III [11].

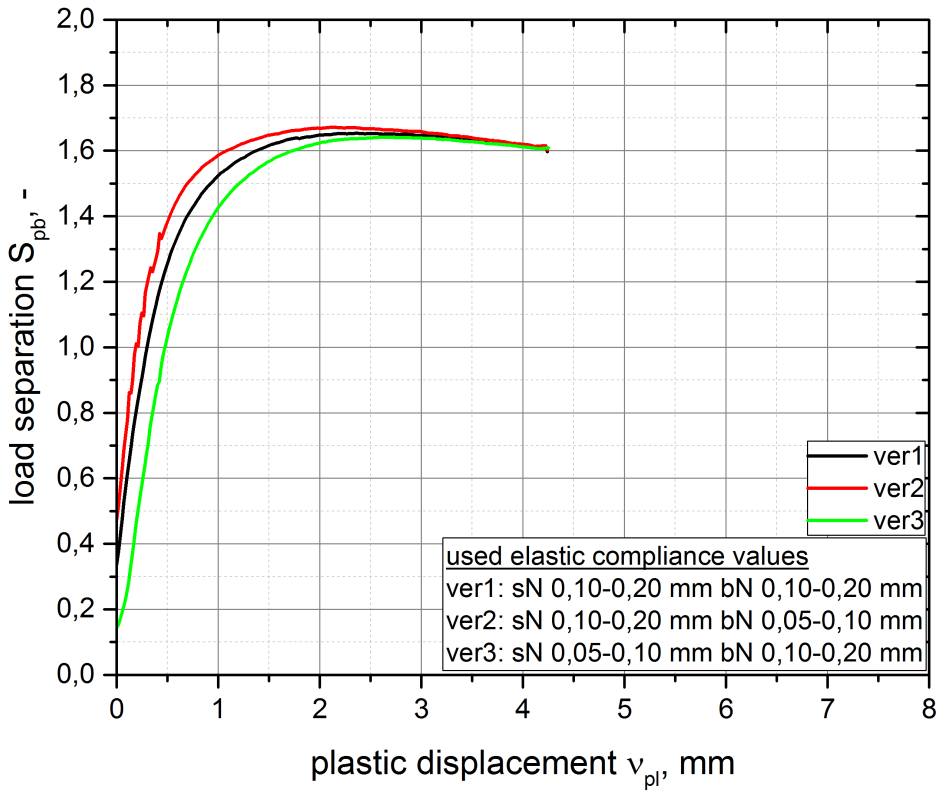

Figure 3.20.: *Load separation parameter S_{pb} depending on the plastic displacement $\nu_{plastic}$ for different used elastic compliance values for PP-B (sN4 with bN1).*

By using the load separation parameter curve it is possible to construct the crack resistance curve for PP-B (sN4 with bN1) shown in Figure 3.21. In the same way as the crack resistance curves of PP-H and PP-R, the different elastic compliance values end up in a different ordinate interception for the crack resistance curve of PP-B (sN4 with bN1). Whereby the slope of the determined crack resistance curves is nearly the same. Compared to the other materials the crack resistance curve of PP-B covers a really low range of determined crack length Δa in the tested specimens. This could be explained by the chosen blunt notched specimens. The blunt notched specimen is only acceptable as reference if there is no crack propagation during testing detected. For

this measurements the tendency of crack propagation in the blunt notched specimen limited the measurable crack length Δa in the sharp notched specimens [11].

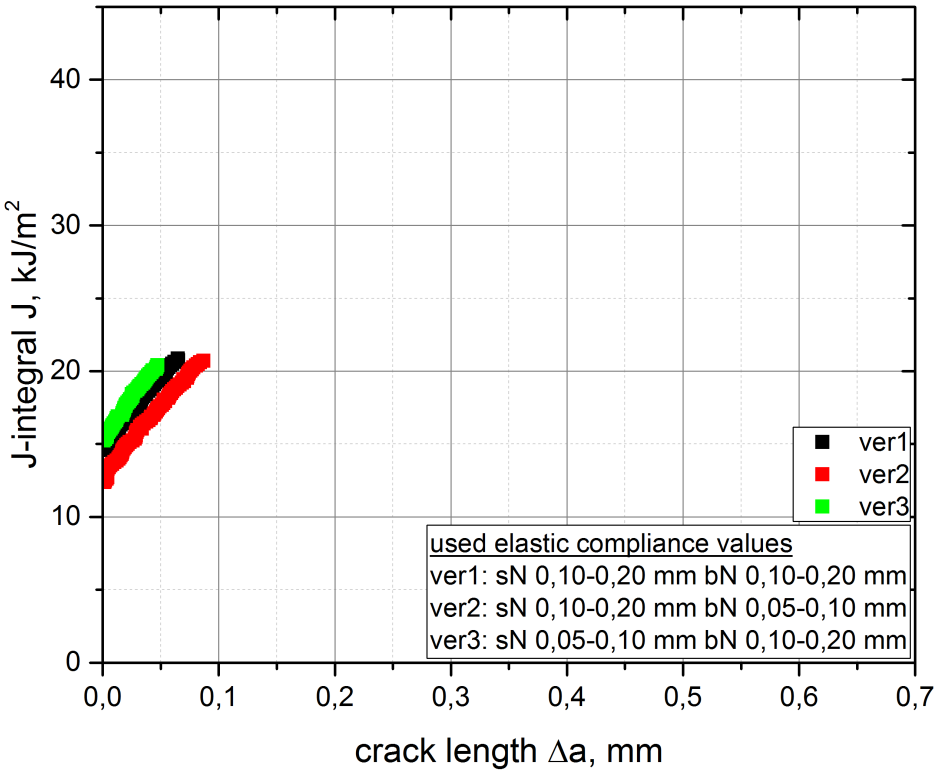

Figure 3.21.: *J-Integral depending on the crack length Δa for different used elastic compliance values for PP-B (sN4 with bN1).*

Load separation method PP-B (sN4 with bN2)

Figure 3.22 shows the load P depending on the plastic displacement $v_{plastic}$ for PP-B (sN4 with bN2). Also influenced by a different chosen elastic compliance C to calculate the plastic displacement $v_{plastic}$, this ends up in three versions (ver1, ver2 and ver3), with different areas for the determination of the elastic compliance (0.1 mm - 0.2 mm or 0.05 mm - 0.1 mm) to present the load curves of PP-B (sN4 with bN2). Both blunt notched samples (bN1 and bN2) of PP-B show almost the same load curve. The

influence of the chosen elastic compliance is also the same as discussed before for PP-B (sN4 with bN1).

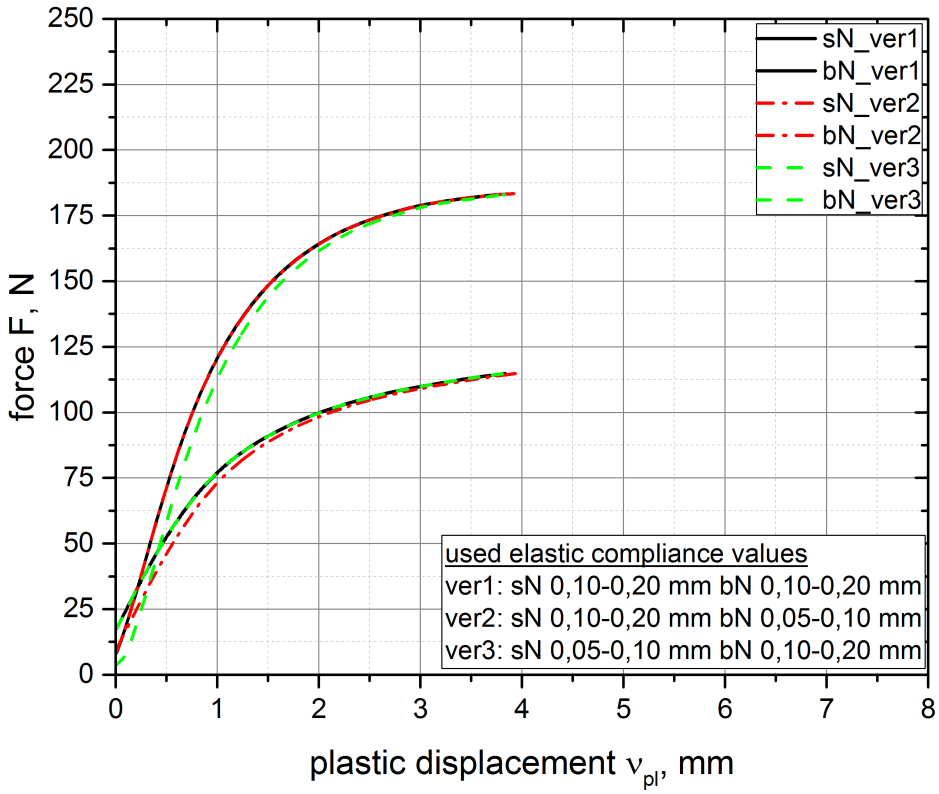

Figure 3.22.: *Load P depending on the plastic displacement $\nu_{plastic}$ for different elastic compliance correction values of PP-B (sN4 with bN2).*

Now it is possible to construct the load separation curves with the influence of different elastic compliance values for PP-B sN4 with bN2 (Figure 3.23). In addition the load separation parameter ends up in the same slope for every version of determined elastic compliance value in region III. But the maximum values of the load separation parameter S_{pb} in region II varies [11].

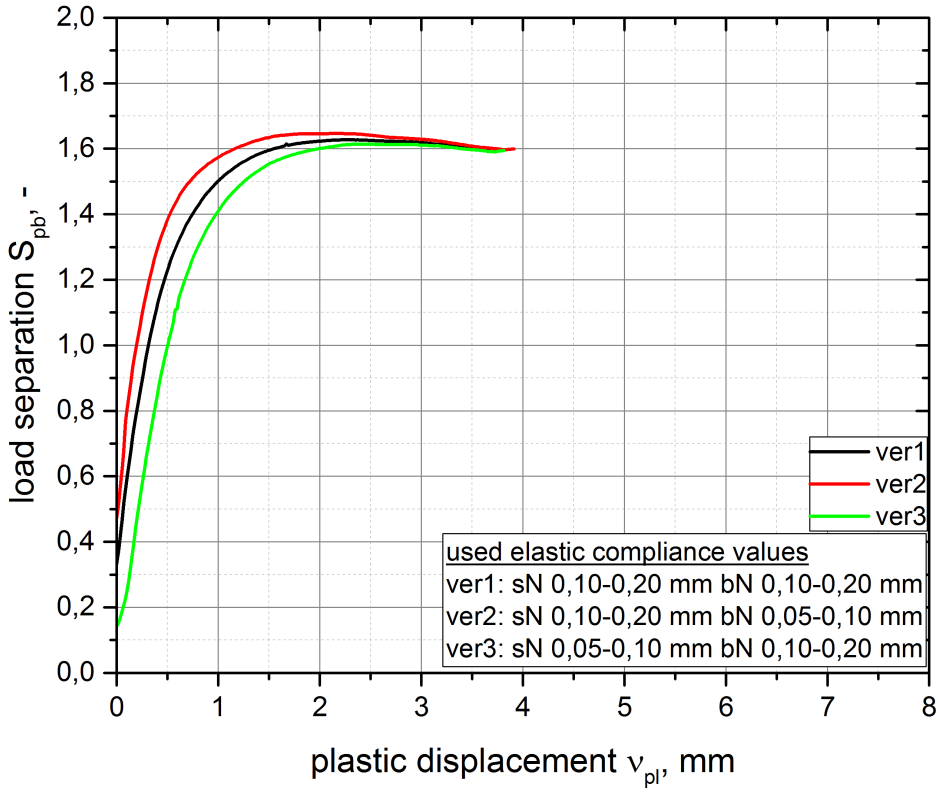

Figure 3.23.: *Load separation parameter S_{pb} depending on the plastic deformation $\nu_{plastic}$ for different used elastic compliance values for PP-B (sN4 with bN2).*

Figure 3.24 presents the crack resistance curve of PP-B (sN4 with bN2) with the influence of different elastic compliance values. The starting point of the three versions of J-R curves is different and varies between 11 kJ/m^2 and 15 kJ/m^2. The difference in the starting point is directly influenced by the maximum value of the load separation method which indicates the beginning of crack growth in the sharp notched specimens. The maximum value of the load separation method depends on the chosen elastic compliance and ends up in different J-R curves. The slope of the determined crack resistance curves of PP-B (sN4 with bN2) is nearly the same.

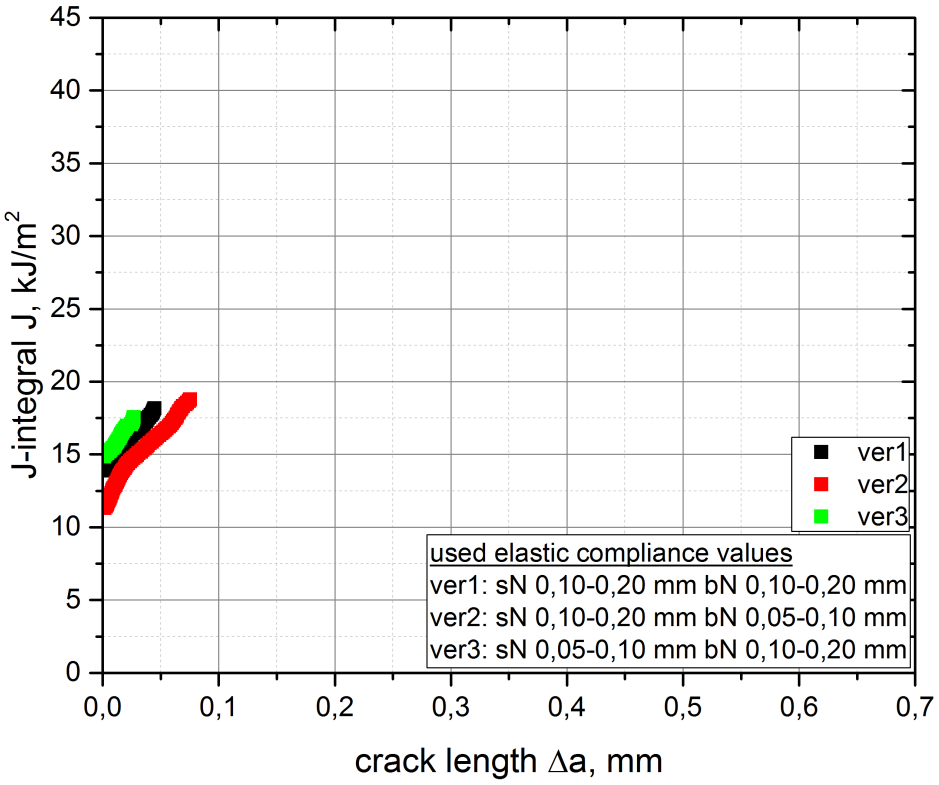

Figure 3.24.: *J-Integral depending on the crack length Δa for different used elastic compliance values for PP-B (sN4 with bN2).*

3.3. Comparison of the multi specimen method and load separation method

The results of the multi specimen method and the results of the load separation method are compared in this section. Therefore, the calculated J-R curve data from the multi specimen method were fitted with a power law function [27]:

$$J = C_1 \Delta a^{C_2} \tag{3.1}$$

Comparison of the two methods for PP-H

The comparison of determined J-R curves for PP-H is shown in Figure 3.25. Here, the data points of the multi specimen method get reduced and fitted by a power law function. In general it is very common that a lot of data points at the multi specimen method are excluded for the fit. This makes the procedure of the multi specimen extremely difficult, and is the main reason for the high specimen consumption. Concerning the load separation method version 1 (the elastic compliance for the sN-specimen and the bN-specimen were chosen between 0.1 mm and 0.2 mm) of the calculated J-R curve was chosen as reference to the multi specimen method.

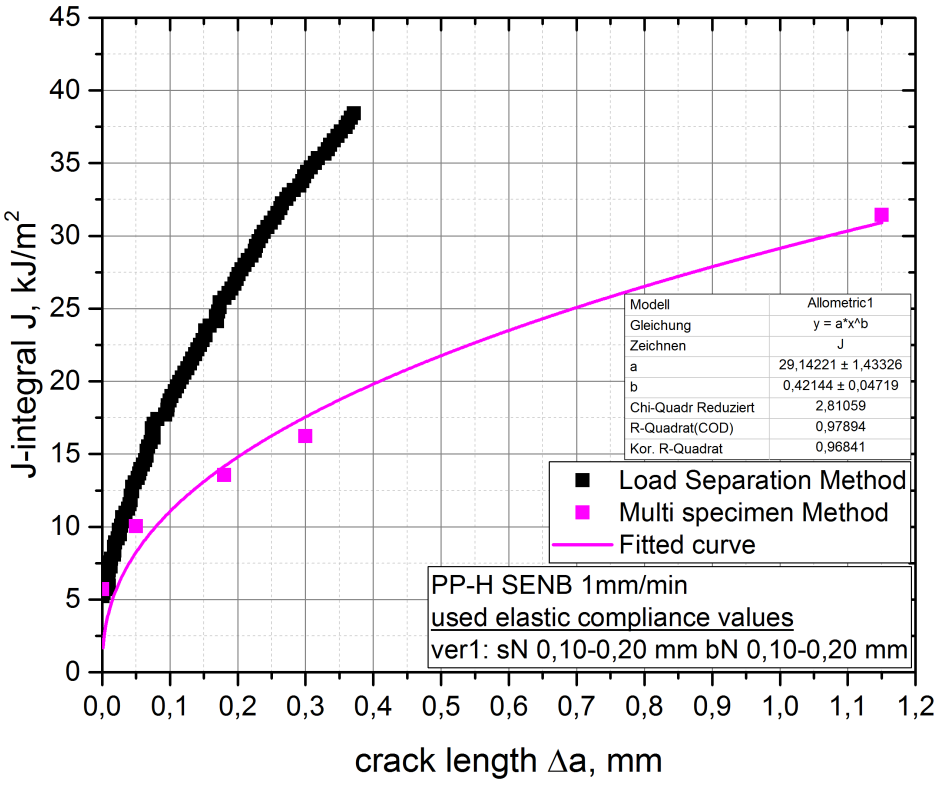

Figure 3.25.: *Comparison of the determined J-Integral depending on the crack length Δa from the multi specimen method and the load separation method of PP-H.*

The crack resistance curve determined with the load separation method for PP-H shows higher values compared to the crack resistance curve determined with the multi specimen method. Both curves start at the same value of the J-Integral around 5 kJ/m^2. The difference between the two methods is a results of a lot influencing factors. As discussed in the theoretical part the determination of the crack length is not always that easy. The comparison of the tested materials is discussed in chapter 3.3.1.

Comparison of the two methods for PP-R

The comparison of the multi specimen method and the load separation method of PP-R is shown in Figure 3.26. In the same way as discussed for PP-H, the data points of the multi specimen method get reduced and in a next step fitted by a power law function. The chosen data points from the multi specimen method and the determination of the actual crack length on the fracture surface of the tested specimens directly influences the fitted J-R curve. For the load separation method, version 1 of determined J-R curves (with a chosen elastic compliance value between 0.1 mm and 0.2 mm) was selected as reference for the comparison.

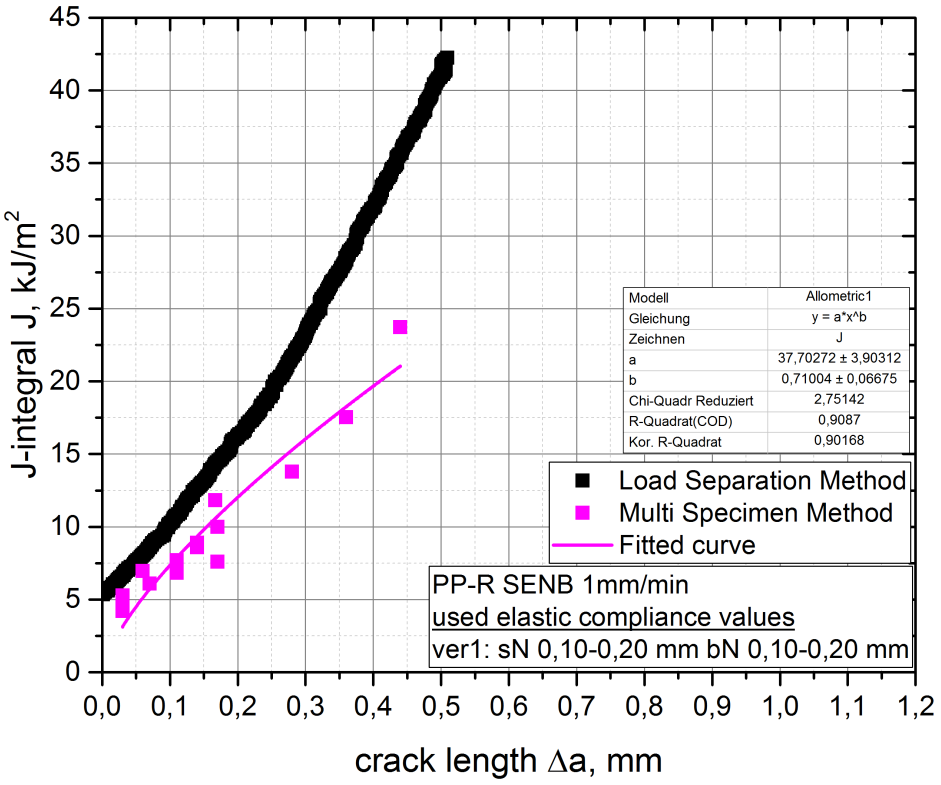

Figure 3.26.: *Comparison of the determined J-Integral depending on the crack length Δa from the multi specimen method and the load separation method of PP-R.*

Both crack resistance curves start nearly at the same value (a J-integral around 5 kJ/m^2). At higher crack lengths, the difference between both curves increases, and the load separation method reaches higher values of J-Integral compared with the J-R curve of the multi specimen method. The reasons for this difference in the crack resistance curve are discussed in chapter 3.3.1.

Comparison of the two methods for PP-B

Figure 3.27 presents the comparison of crack resistance curve of the multi specimen method and the load separation method for PP-B. Therefore the data points of the multi specimen method get reduced and fitted by a power law function according to [27].

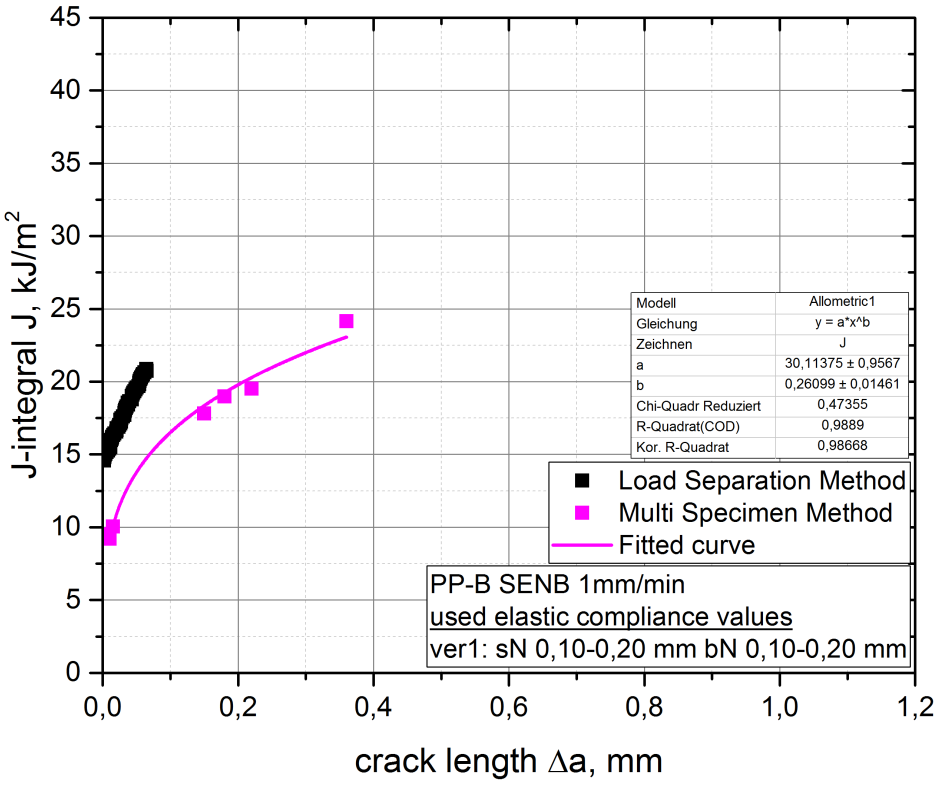

Figure 3.27.: *Comparison of the determined J-Integral depending on the crack length Δa from the multi specimen method and the load separation method of PP-B.*

The J-R curve of both methods show different staring values. The crack resistance curve of the load separation method starts at a J-Integral around 14 kJ/m^2 and the J-R curve of the multi specimen method around 9 kJ/m^2. Generally, the multi specimen method shows lower values of the crack resistance curve in comparison with the load separation method. The difference between both methods is described by a lot of influencing factors discussed in the next chapter.

3.3.1. Discussion of the comparison and material ranking

First of all the multi specimen method is directly influenced by the determination of the actual crack length. The single specimen method characterizes the crack growth

during testing indirect with the help of the load separation parameter S_{pb} and a parameter m_s. Furthermore, the determination of the parameter m_s is another strong influence on the resulting J-R curve. This influences are widely debated in literature and interesting for further investigations [27].

Finally, it was possible to investigate the initiation toughness $J_{0.2}$ (the J-Integral at a crack length Δa of 0.2 mm) for every tested material. Additionally, the slope of the J-R-curve $dJ/d(\Delta a)_{0.2}$ at a crack length Δa of 0.2 mm was determined as a further parameter to characterize the fracture behaviour of the tested materials. The values were taken from the multi specimen J-R-curve. The load separation method was used to characterize a further parameter m_s to rank the tested types of Polypropylene (see chapter 3.4). Hence, PP-B shows the highest value of initiation toughness $J_{0.2}$ (20 kJ/m^2), followed by PP-H ($J_{0.2}$ = 15 kJ/m^2) and PP-R ($J_{0.2}$ = 12.5 kJ/m^2). Concerning the mentioned slope of the J-R-curve $dJ/d(\Delta a)_{0.2}$, PP-R shows the highest value ($dJ/d(\Delta a)_{0.2}$ = 42,7 N/mm^2). For PP-H a value of 31,1 N/mm^2 for $dJ/d(\Delta a)_{0.2}$ was determined an PP-B shows the lowest slope of the J-R curve ($dJ/d(\Delta a)_{0.2}$ = 25.8 N/mm^2). As a comparison, PP-R implifies the lowest initiation toughness $J_{0.2}$ but the highest slope of the J-R-curve $dJ/d(\Delta a)_{0.2}$ of the tested materials. Whereas PP-B displays the highest initiation toughness $J_{0.2}$ with the lowest value for the slope $dJ/d(\Delta a)_{0.2}$ and PP-H is in between. It is not defined whether the initiation toughness $J_{0.2}$ or the slope $dJ/d(\Delta a)_{0.2}$ is more significant as a fracture toughness parameter for a non linear elastic plastic material [8].

3.4. Determination of the normalized load separation curve

To compare the different tested materials concerning the mentioned parameter m_s, which indicates the crack advancement produced per unit of plastic displacement, the normalized load separation curve was determined and is shown in Figure 3.28.

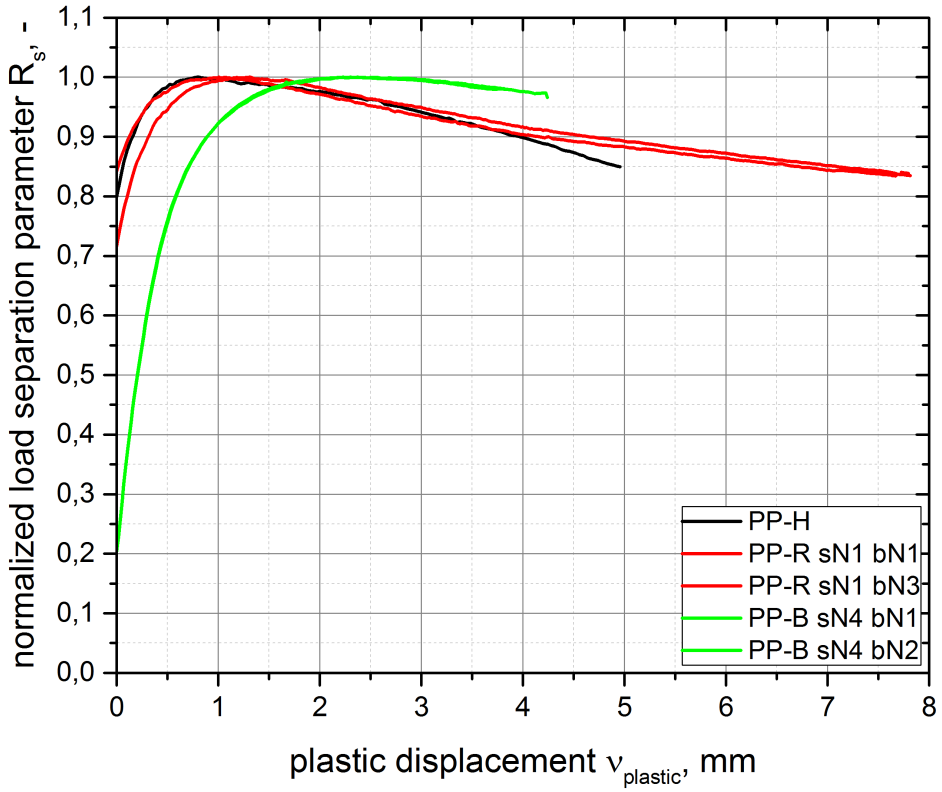

Figure 3.28.: *Comparison of the determined normalized load separation parameter R_s depending on the plastic displacement $\nu_{plastic}$ for PP-H, PP-R and PP-B.*

The three tested materials differ in region I and region II of the normalized load separation curves and also the slope in region III is different for PP-H, PP-R and PP-B. This indicates the key role of the slope in region III as a criterion to rank different materials concerning their fracture behaviour. For a detailed discussion the slope in region three was determined by using the parameter m_s and the results are shown in Figure 3.29 [4].

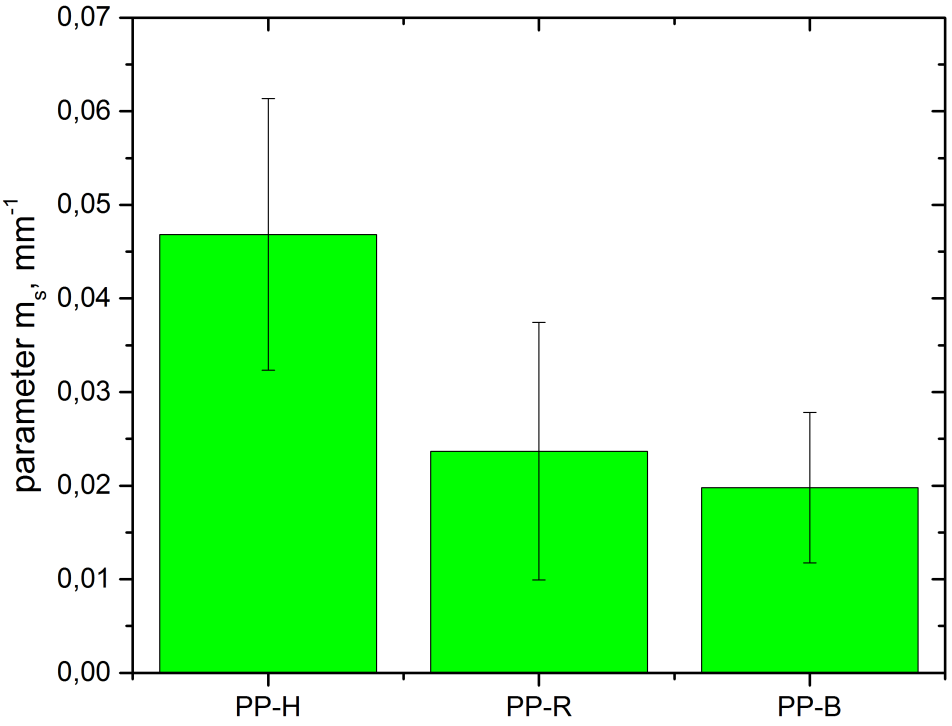

Figure 3.29.: *Comparison of the parameter m_s for PP-H, PP-R and PP-B.*

Generally the parameter m_s can cover a wide range of values. For example nearly zero, when the normalized load separation curve is constant in region III. This indicates no crack propagation with increasing plastic displacement and the fracture process is dominated by blunting processes. Or a value of nearly 1 mm^{-1} for the parameter m_s which represents a relative high crack propagation per unit of plastic displacement. For materials with a high m_s parameter it is possible to determine a crack resistance curve with the help of the methods of non linear EPFM but it is also possible to evaluate a crack resistance curve with the methods of LEFM. Hence, the parameter m_s is extremely useful to check the application of LEFM or EPFM methods to characterize the fracture behaviour of ductile polymers [4].

The parameter m_s was determined in region III of the normalized load separation curve (region of stable crack growth, after the maximum value of the normalized load separation parameter R_s). For the three types of Polypropylene an average value of the parameter m_s and a standard deviation was calculated which covers the whole region of stable crack growth. PP-H show a value of $0.05\,mm^{-1}$ for the parameter m_s with a standard deviation of $0.01\,mm^{-1}$. The results for PP-R are a bit lower ($0.02\,mm^{-1}$ for the parameter m_s with a standard deviation of $0.01\,mm^{-1}$) compared to the results of PP-H. Additionally PP-B shows a lower value of $0.02\,mm^{-1}$ for the parameter m_s with a standard deviation of $0.01\,mm^{-1}$. There exist some results of the parameter m_s in literature [4], for example ABS show a value of $0.25\,mm^{-1}$ for the parameter m_s and HIPS a value of $0.33\,mm^{-1}$. There is no information about different sorts of Polypropylene. But in general the parameter m_s of Polypropylene should be lower compared to ABS and HIPS, because Polypropylene shows a tougher material behaviour. Hence, the determined values of the parameter m_s for the different sorts of Polypropylene imply for further investigations [4].

4. Conclusion and Outlook

It is common to use extremely tough types of Poylpropylene for applications which requires a high crack resistance. Hence, it is important to examine and rank the fracture behaviour with the help of a crack growth parameter. In the case of extremely tough Polypropylene the methods of the non linear elastic plastic fracture mechanics are necessary. The focus of this study was the examination of different J-Integral methods to determine a crack resistance curve for tough Polypropylene materials.

There exists several methods for a practical application of the J-Integral. One of the most common procedures is the multi specimen method developed by the Technical Committee 4 of European Structural Integrity Society, ESIS TC4, on "Polymers and Polymeric Composites. Within this study several identical specimens are loaded up to different amounts of displacement and immediately afterwards unloaded without complete fracturing. The different amounts of displacement produce different amounts of crack propagation Δa in the specimens. To determine the actual crack length Δa directly from the crack surface the specimens get cooled in liquid nitrogen and cryo fractured. Finally it is possible to construct a crack resistance curve (J-R curve) with the calculated J-Integral of the measured load-displacement curve and the determined crack length Δa from the crack surface of the specimens. There are a lot of influencing factors concerning the determination of the J-R curve via the multi specimen method like the exact determination of the crack length Δa. The results of this study demonstrate the strong influence of the measured crack length Δa to the resulting J-R curve. For a representative crack resistance curve a large amount of specimens are required. The high material consumption and specimen preparation

as well as difficulties with correct crack length detection push the development of alternative procedures to characterize the non linear elastic plastic material behaviour of polymers [8].

The development of indirect methods (single specimen methods) for the characterization of the crack resistance curve is strongly promoted at the moment. In this study the load separation method, first presented by Sharobeam and Landes, was used. Based on the theoretical conditions, only two specimens are required (a sharp notched and a blunt notched specimen). Whereby both specimens are tested but only in the sharp notched specimen crack propagation is allowed. In a next step a load separation parameter S_{pb} is defined as a ratio of the load of the sharp notched and the load of the blunt notched specimen during testing. These parameter depends on the plastic displacement $v_{plastic}$ which is determined from the measured displacement subtracing an elastic compliance value C times the load P. With the help of the determined load separation parameter curve and the final crack length of the crack surface of the sharp notched specimen, it is possible to calculate the crack propagation in the sharp notched specimen during testing. Finally it is possible to construct the crack resistance curve (J-R-curve) with the calculated J-integral of the measured load displacement curve of the sharp notched specimen and the determined crack length Δa from the load separation parameter curve. Concerning the load separation method, there are more influencing parameters caused by the procedure itself. First of all the influence of the crack growth onset, which is directly connected to the maximum value of the load separation parameter S_{pb} and the evaluation of the crack propagation in the sharp notched specimen with the help of only the final crack length measured on the crack surface. Furthermore the chosen blunt notched specimen, which acts as reference to the sharp notched specimen, influences the determination of the J-R curve. In this study the influence of the chosen elastic compliance value to determine the plastic displacement $v_{plastic}$ is discussed in detail. Especially in the first and the second region of the load separation parameter curve the influence of the chosen elastic compliance value is significant and ends up in variations in the J-R curve [11].

Additionally the determined J-R curves from the multi specimen method and the load separation method were compared. They show an equal range of the calculated J-Integral but the determined crack length Δa displays differences. Hence, it is necessary to improve the characterization of the actual crack length Δa.

Finally, the parameter m_s was determined of the slope in region III of the normalized load separation curve. This parameter m_s indicates the crack advancement produced per unit of plastic displacement. Concerning to literature [4] the parameter m_s depends on the material and indicates a key role in the fracture characterization of ductile polymers. It is possible to use the parameter m_s as a criterion for a correct application of the J-Integral. The tested Polypropylene types show a relative low parameter m_s. In this case the application of the J-Integral as fracture criterion to rank types of tough Polypropylene should be possible, although already challenging.

5. Bibliography

[1] B.D. Agarwal. J-integral as fracture criterion for short fibre composites: an experimental approach. *Engineering Fracture Mechanics*, 1984(19):678–684.

[2] J.R. Rice. A path independent integral and the approximate analysis of strain concentration by notches and cracks. *Journal of applied mechanics*, 1968(35):379–386.

[3] P. Frontini. On the applicability of the load separation criterion to acrylonitrile/butadiene/styrene terpolymer resins. *Polymer;*, 1996(37):4033–4039.

[4] F. Baldi. Application of the load separation criterion in j-testing of ductile polymers: A round-robin testing exercise. *Polymer Testing*, (44):72–81, 2015.

[5] ESIS Publication 28, editor. *Fracture mechanics testing methods for polymers adhesives and composites*. Oxford, UK, 2001.

[6] F. Baldi. On the applicability of the load separation criterion in determining the fracture resistance (jic) of ductile polymers at low and high loading rates. *Int J Fract*, (165):105–119, 2010.

[7] F. Baldi. On the determination of the point of fracture initiation by the load separation criterion in j-testing of ductile polymers. *Polymer Testing*, (32):1326–1333, 2013.

[8] G. E. Hale. J-fracture toughness of polymers at slow speed. *Fracture mechanics testing methods for polymers*, pages 123–157, 2001.

[9] X.K. Zhu. J-integral resistance curve testing and evaluation. *Journal of Zhejiang University Science A*, 2009(10):1541–1560.

[10] N. Leon. The post-yield fracture of a ductile polymer film: Notch quality, essential work of fracture, crack tip opening displacement, and j-integral. *Engineering Fracture Mechanics*, 2017(173):21–31.

[11] A. Salazar. The use of the load separation parameter spb method to determine the j–r curves of polypropylenes. *Polymer Testing*, (27):977–984, 2008.

[12] F. Baldi. High-rate j-testing of toughened polyamide 6/6: Applicability of the load separation criterion and the normalization method. *Engineering Fracture Mechanics*, 2005(72):2218–2231.

[13] J. R. Rice. Mathematical analysis in the mechanics of fracture. *Mathematical Fundamentals*, 1968(Vol 2):191–311.

[14] H. Ernst. Analysis of load-displacement relationship to determine j-r curve and tearing instability material properties. *American Society of Testing and Materials*, 1979:581–599.

[15] X.-K. Zhu. Review of fracture toughness (g, k, j, ctod, ctoa) testing and standardization. *Engineering Fracture Mechanics*, (85):1–46, 2012.

[16] J. A. Begley and J. D. Landes. The j-integral as a fracture criterion. *National Symposium on Fracture mechanics*, 1971(Part II, ASTM STP 514):1–20.

[17] J.R. Rice and G. F. Rosengren. Plane strain deformation near a crack tip in a power-law hardening material. *Journal of the mechanics and physics of solids*, 1968(Vol 16):1–12.

[18] N.K. Simha. J-integral and crack driving force in elastic–plastic materials. *Journal of the mechanics and physics of solids*, 2008(56):2879–2895.

[19] J.R. Rice. Some furhter results of j-integral analysis and estimates. *Progress in Flaw Growth and Fracutre Toughness Testing*, 1973(536):231–245.

[20] J. W. Hutchinson. Crack-tip singularity fields in nonlinear fracture mechanics: a survey of current status. *Advances in Fracture Research*, 1982(Vol. 6).

[21] J.W. Hutchinson. Singular behaviour at the end of a tensile crack in a hardening material. *Journal of the mechanics and physics of solids*, 1968(16):13–31.

[22] J. Hebel, J. Hohe, V. Friedmann, and D. Siegele. Experimental and numerical analysis of in-plane and out-of-plane crack tip constraint characterization by secondary fracture parameters. *Int J Fract*, 2007(146):173–188.

[23] M.L. Williams. On the stress distribution at the base of a stationary crack. *Journal of applied mechanics*, 1957(24):109–114.

[24] K. S. Woo and C. H. Hong. J-integral and fatigue life computations in the incremental plasticity analysis of large scale yielding by p-version of f.e.m. *Structural Engineering & Mechanics*, 2004.

[25] O. Kolednik. A new view on j-integrals in elastic–plastic materials. *Int J Fract*, 2014(187):77–107.

[26] M.A. Haque. Visualization of crack blunting using secondary fluorescence in soft polymers. *Polymer Testing*, 2008(27):404–411.

[27] M.Ll. Maspoch. Fracture characterization of ductile polymers through methods based on load separation. *Polymer Testing*, 2009(28):204–208.

[28] Patricia María Frontini. Non linear fracture mechanics of polymers: Load separation and normalization methods. *Engineering Fracture Mechanics*, (79):389–414, 2012.

[29] Patricia M. Frontini. A simple method for j-r curve determination in abs polymers. *Polymer Testing*, (14):85–96, 1995.

[30] Patricia M. Frontini. The use of load separation criterion and normalization method in ductile fracture characterization of thermoplastic polymers. *Journal of polymer science Part B Polymer Physics*, 1996(34):1869–1880.

[31] J. Wainstein. Influence of the calibration points on the spb parameter behavior. *Journal of testinng and evaluation*, 2007(35).

[32] P.M. Frontini. High rate toughness of ductile polymers. *Engineering Fracture Mechanics*, (74):2070–2083, 2007.

[33] F. J. Arbeiter. Influence of molecular structure and reinforcement on fatigue behavior of tough polypropylene materials. *Journal of applied polymer science*, 2016.

[34] A. Salazar. Influence of the notch sharpening technique on the fracture toughness of bulk ethylene–propylene block copolymers. *Polymer Testing*, (29):49–59, 2010.

[35] J. Wainstein. J-r curve determination using the load separation parameter spb method for ductile polymers. *Polymer Testing*, (23):591–598, 2004.

[36] A. Salazar. Determination of fracture toughness of propylene polymers at different operating temperatures. *Engineering Fracture Mechanics*, (126):87–107, 2014.

[37] P. Frontini. The effects of specimen size and testing conditions on fracture toughness evaluation of polypropylene homo polymer. *Polymer Engineering and science*, 2001(41):1803–1814.

[38] A. Salazar. Fracture toughness of high density polyethylene: Fatigue precracking versus femtolaser, razor sharpening and broaching. *Engineering Fracture Mechanics*, (149):199–213, 2015.

[39] L. A. Fasce. Polypropylene modified with elastomeric metallocene- catalyzed polyolefin blends: Fracture behavior and development of damage mechanisms. *JOurnal of polymer science;*, 2004(42):1075–1089.

[40] C.J.G. Plummer. Influence of the loading rate on the fracture resistance of isotactic polypropylene and impact modified isotactic polypropylene. *Polymer;*, 1999(41):3809–3819.

[41] R. G. COCCO. Fracture toughness of polymers in the ductile-to-brittle transition region: Statistical approach and lower bound determination. *Wiley InterScience*, 2005.

[42] A. Salazar. The role of notch sharpening on the j-fracture toughness of thermoplastic polymers. *Engineering Fracture Mechanics*, 2013(101):10–22.

[43] L. Fasce. Mechanical evaluation of propylene polymers under static and dynamic loading conditions. *Journal of applied polymer science*, 1999(74):2681–2693.